Iterative Solvers for Large Linear Systems
Part IV: Introduction to Multigrid Methods

Andreas Meister

University of Kassel, Department of Analysis and Applied Mathematics

Outline

- Basics of Iterative Methods
- Splitting schemes
  - Jacobi scheme and Gauß-Seidel method
  - Relaxation methods
- Methods for symmetric, positive definite matrices
  - Method of steepest descent
  - Method of conjugate directions
  - CG scheme

Outline

- Multigrid Method
  - Smoother, Prolongation, Restriction
  - Twogrid Method and Extension
- Methods for non-singular Matrices
  - GMRES
  - BiCG, CGS and BiCGSTAB
- Preconditioning
  - ILU, IC, GS, SGS, ...

Model problem: Poisson's equation

Given: $\Omega = (0,1)$ and $f \in C(\Omega, \mathbb{R})$

Sought: $u \in C^2(\Omega, \mathbb{R}) \cap C(\overline{\Omega}, \mathbb{R})$ with

$$\begin{aligned} -u''(x) &= b(x) \quad \text{for } x \in \Omega, \\ u(x) &= 0 \quad \text{for } x \in \partial\Omega = \{0, 1\}. \end{aligned}$$

Mesh hierarchy: $\Omega_\ell := \Omega_{h_\ell} = \{ jh_\ell \mid j = 1, \ldots, 2^{\ell+1} - 1 \}$ $\ell = 0, 1, \ldots$

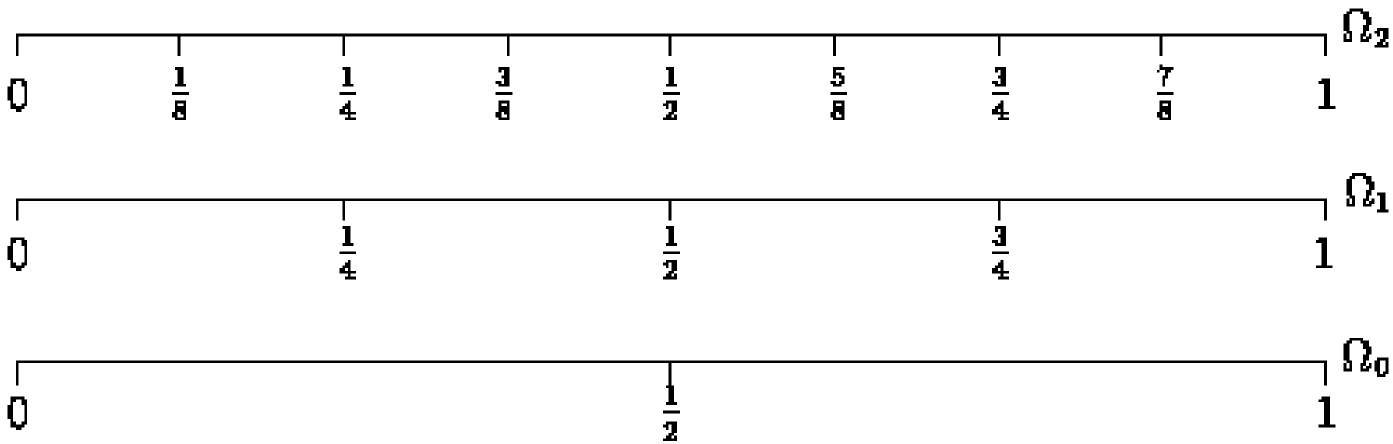

$$N_\ell := 2^{\ell+1} - 1, \quad h_\ell = 2^{-\ell} h_0, \quad h_0 = 1/2$$

Model problem: Poisson's equation

Approximation: Utilizing $u_j^\ell := u(jh_\ell)$ yields

$$-u''(jh_\ell) \approx \frac{-u_{j+1}^\ell + 2u_j^\ell - u_{j-1}^\ell}{h_\ell^2}$$

Linear system of equations:

$$\boldsymbol{A}_\ell \boldsymbol{u}^\ell = \boldsymbol{b}^\ell$$

with

$$\boldsymbol{A}_\ell = \frac{1}{h_\ell^2} \begin{pmatrix} 2 & -1 & & & \\ -1 & 2 & -1 & & \\ & \ddots & \ddots & \ddots & \\ & & \ddots & \ddots & -1 \\ & & & -1 & 2 \end{pmatrix} \in \mathbb{R}^{N_\ell \times N_\ell}, \quad \boldsymbol{u}^\ell = \begin{pmatrix} u_1^\ell \\ u_2^\ell \\ \vdots \\ u_{N_\ell}^\ell \end{pmatrix}.$$

Fourier modes

Eigenfunctions of the corresponding boundary value problem

$$u'' = \alpha u, \; u(0) = u(1) = 0 \quad \text{are} \quad u(x) = c \sin(j\pi x), \; j \in N, \; c \in R.$$

Definition of the Fourier modes

The vectors

$$\boldsymbol{e}^{\ell,j} = \sqrt{2h_\ell} \begin{pmatrix} \sin j\pi h_\ell \\ \vdots \\ \sin j\pi N_\ell h_\ell \end{pmatrix} \in \mathbb{R}^{N_\ell}, \quad j = 1, \ldots, N_\ell$$

are called Fourier modes.

Properties of the Fourier modes

- Orthonormal basis of $\mathbb{R}^{N_\ell}$
- Discrete, equidistant sampling of the eigenfunctions
- Eigenvectors

$$\boldsymbol{A}_\ell \boldsymbol{e}^{\ell,j} = \lambda^{\ell,j} \boldsymbol{e}^{\ell,j}, \quad \lambda^{\ell,j} = 4h_\ell^{-2} \sin^2\left(\frac{j\pi h_\ell}{2}\right), \quad j = 1, \ldots, N_\ell.$$

Jacobi relaxation method

We consider the linear system

$$\boldsymbol{A}_\ell \boldsymbol{u}^\ell = \boldsymbol{b}^\ell \quad \text{w.r.t. the mesh} \quad \Omega_\ell$$

using the usual splitting ansatz:

$$\boldsymbol{A}_\ell = \boldsymbol{B}_\ell + (\boldsymbol{A}_\ell - \boldsymbol{B}_\ell), \boldsymbol{B}_\ell = \boldsymbol{D}_\ell = \mathrm{diag}\{\boldsymbol{A}_\ell\} = \mathrm{diag}\{2h_\ell^{-2}\}.$$

$$\begin{aligned}
\boldsymbol{u}^\ell_{m+1} &= \boldsymbol{u}^\ell_m + \tilde{\omega} \boldsymbol{D}_\ell^{-1} \left(\boldsymbol{b}^\ell - \boldsymbol{A}_\ell \boldsymbol{u}^\ell_m \right) \\
&= \boldsymbol{u}^\ell_m + \omega h_\ell^2 \left(\boldsymbol{b}^\ell - \boldsymbol{A}_\ell \boldsymbol{u}^\ell_m \right), \quad \omega = \tilde{\omega}/2 \\
&= \underbrace{\left(\boldsymbol{I} - \omega h_\ell^2 \boldsymbol{A}_\ell \right)}_{\boldsymbol{M}_\ell(\omega)} \boldsymbol{u}^\ell_m + \underbrace{\omega h_\ell^2 \boldsymbol{I}}_{\boldsymbol{N}_\ell(\omega)} \boldsymbol{b}^\ell
\end{aligned}$$

Does an interrelationship between error and Fourier modes exist?

Jacobi relaxation method

Introducing the exact solution

$$\boldsymbol{u}^{\ell,*} = \boldsymbol{A}_\ell^{-1}\boldsymbol{b}^\ell$$

yields (due to the consistency) with $\boldsymbol{u}_0^\ell - \boldsymbol{u}^{\ell,*} = \sum_{j=1}^{N_\ell} \alpha_j \boldsymbol{e}^{\ell,j}$

$$\begin{aligned}
\boldsymbol{u}_1^\ell - \boldsymbol{u}^{\ell,*} &= \boldsymbol{M}_\ell(\omega)\boldsymbol{u}_0^\ell + \boldsymbol{N}_\ell(\omega)\boldsymbol{b}^\ell - \left(\boldsymbol{M}_\ell(\omega)\boldsymbol{u}^{\ell,*} + \boldsymbol{N}_\ell(\omega)\boldsymbol{b}^\ell\right) \\
&= \boldsymbol{M}_\ell(\omega)\left(\boldsymbol{u}_0^\ell - \boldsymbol{u}^{\ell,*}\right) = \sum_{j=1}^{N_\ell} \alpha_j \lambda^{\ell,j}(\omega)\boldsymbol{e}^{\ell,j}.
\end{aligned}$$

Finally

$$\boldsymbol{u}_m^\ell - \boldsymbol{u}^{\ell,*} = \sum_{j=1}^{N_\ell} \alpha_j \left[\lambda^{\ell,j}(\omega)\right]^m \boldsymbol{e}^{\ell,j} \text{ for } m = 0, 1, \ldots$$

with

$$\lambda^{\ell,j}(\omega) = 1 - 4\omega \sin^2\left(\frac{j\pi h_\ell}{2}\right), \quad j = 1, \ldots, N_\ell$$

since $\boldsymbol{M}_\ell(\omega) = (\boldsymbol{I} - \omega h_\ell^2 \boldsymbol{A}_\ell)$

Error analysis of the classical Jacobi method ($\omega = 1/2$)

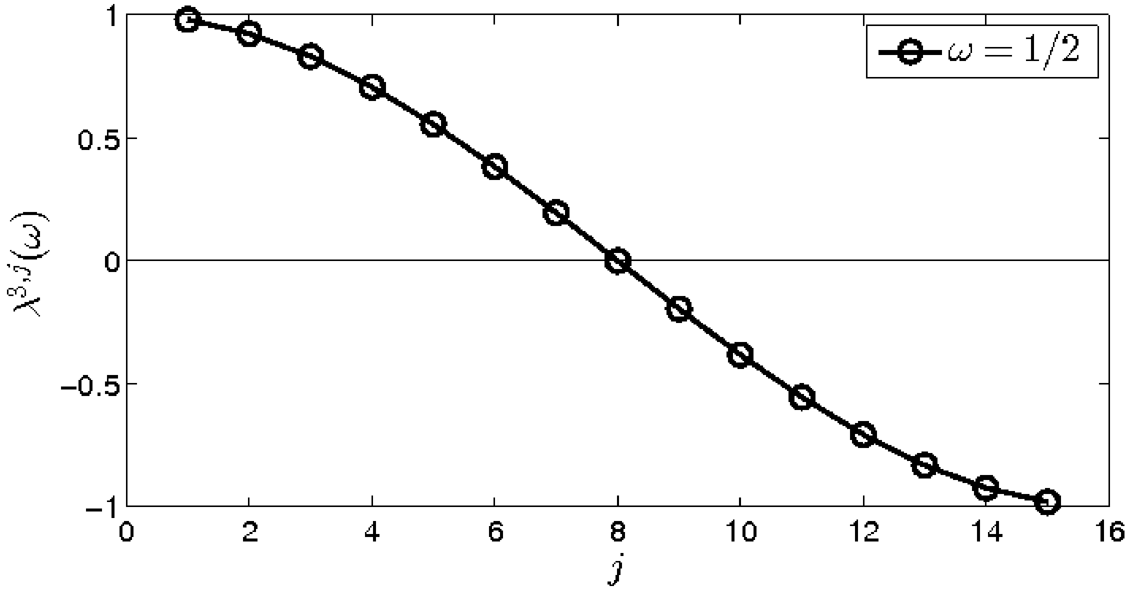

- Significant damping of medium frequencies.
- Almost no damping of small and high frequencies.
- Refinement of the grid $\rightarrow$ degradation of the convergence rate.
- Due to $\lambda^{\ell,1}(1/2) = \lambda_{max} = -\lambda_{min} = -\lambda^{\ell,N_\ell}(1/2)$ no acceleration by means of relaxation is possible.

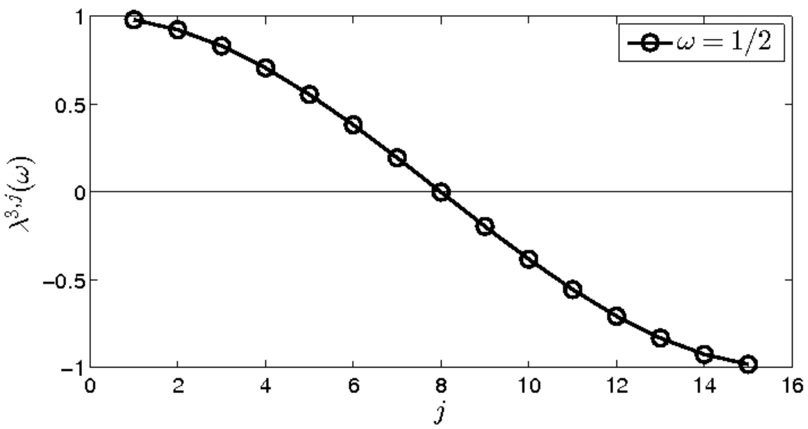

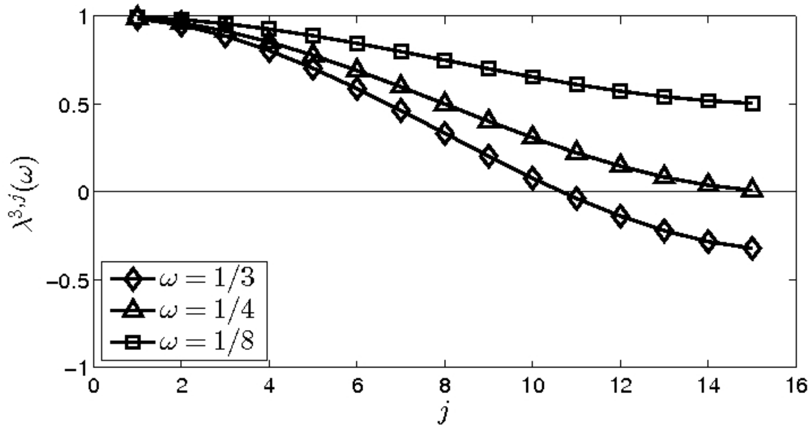

Convergence test:

- Consider the grid Ω_3 and the corresponding Fourier modes $\boldsymbol{e}^{3,j}$, $j = 1, \ldots, 15$.
- For each Fourier mode and each relaxation parameter ω count the number of iterations m necessary to satisfy

$$\|\boldsymbol{M}_J(\omega)^m \boldsymbol{e}^{\ell,j}\|_2 \leq 10^{-2} \underbrace{\|\boldsymbol{e}^{\ell,j}\|_2}_{=1} = 10^{-2}$$

Variation of the relaxation parameter

Classical Jacobi method

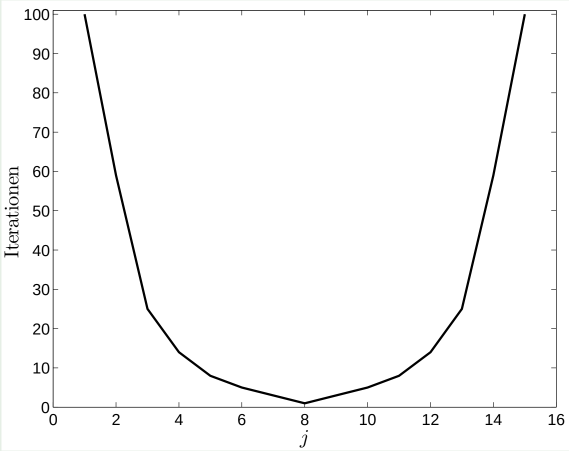

Relaxation parameter $\omega = 1/3$

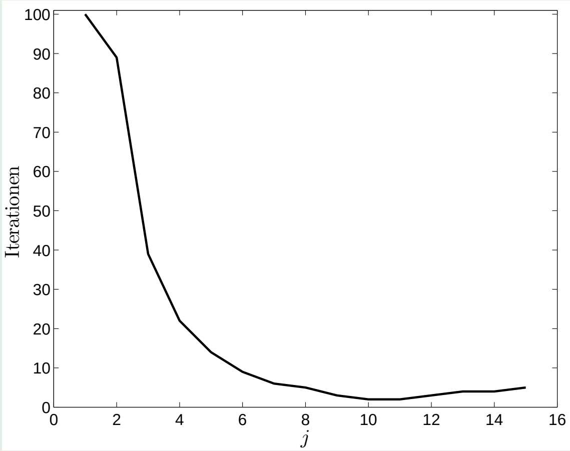

Relaxation parameter $\omega = 1/4$

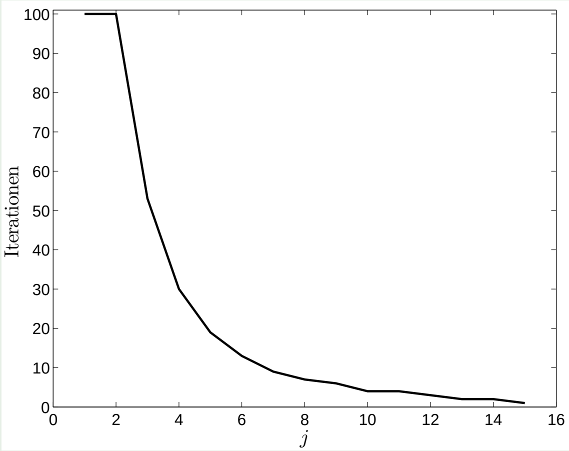

Relaxation parameter $\omega = 1/8$

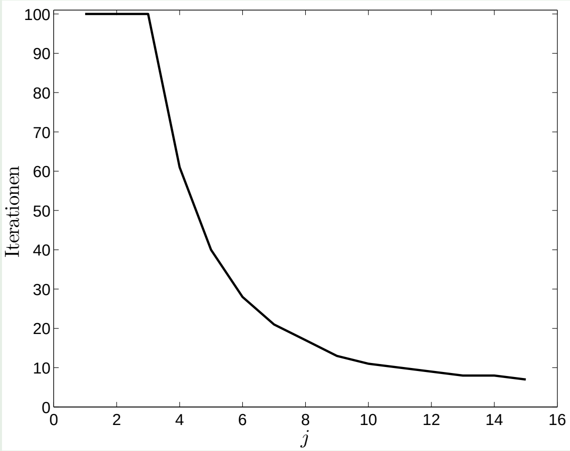

Damped Jacobi method ($\omega = 1/4$)

Development of the error

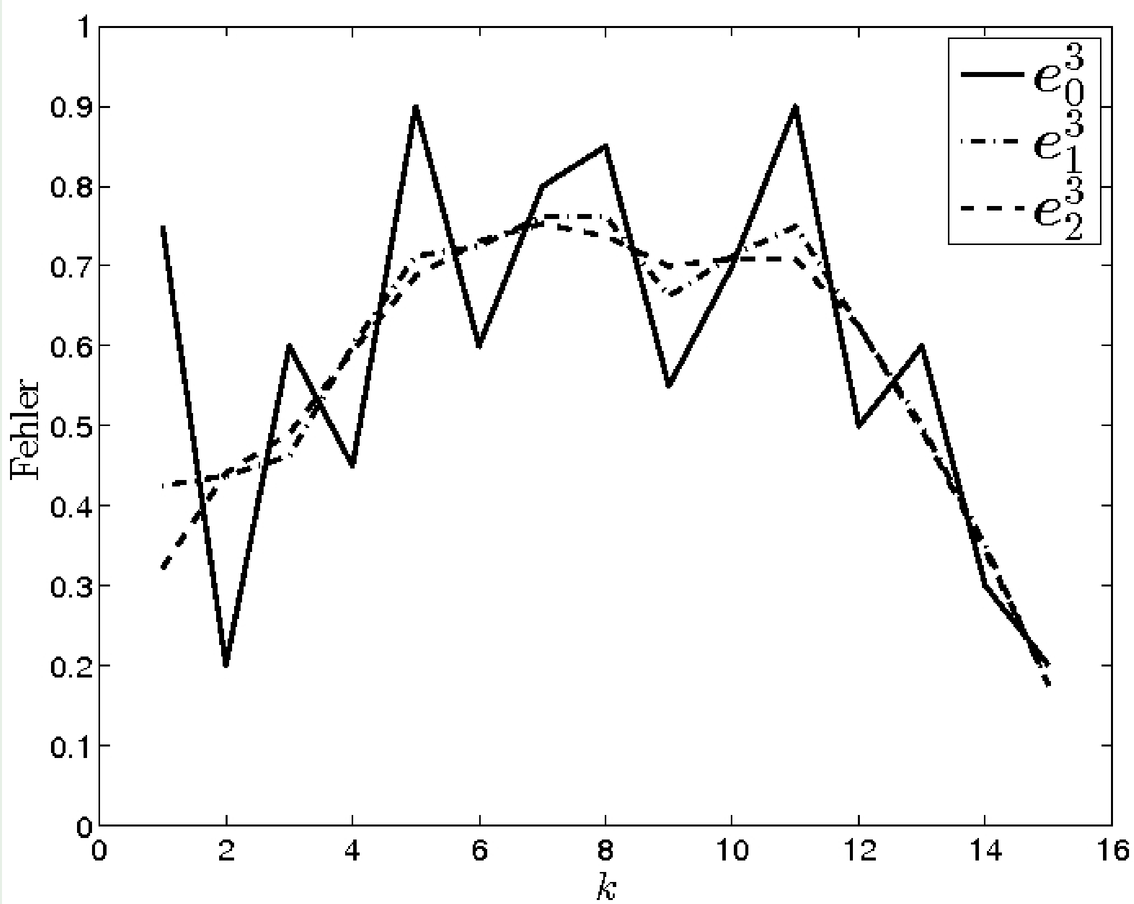

$$\mathbf{e}_0^3 := (0.75,\ 0.2,\ 0.6,\ 0.45,\ 0.9,\ 0.6,\ 0.8,\ 0.85,\ 0.55,\ 0.7,\ 0.9,\ 0.5,\ 0.6,\ 0.3,\ 0.2)^T \in \mathbb{R}^{15}$$

Basic Idea of the Two Grid Method

- Significant damping of high error frequencies on the fine grid Ω_ℓ (Fourier modes $\boldsymbol{e}^{\ell,j}$, j close to N_ℓ)
- Approximation of long wave errors on $\Omega_{\ell-1}$
- Correction of the approximate solution on the fine grid Ω_ℓ using the error approximation on the coarse grid $\Omega_{\ell-1}$
- Basically required operators:
  - Smoother on $\Omega_\ell \rightarrow$ Damped Jacobi method
  - Mapping from Ω_ℓ to $\Omega_{\ell-1} \rightarrow$ Restriction
  - Solver on $\Omega_{\ell-1} \rightarrow$ Direct or iterative method
  - Mapping from $\Omega_{\ell-1}$ to $\Omega_\ell \rightarrow$ Prolongation
  - Correction step on Ω_ℓ

Mapping from Ω_ℓ to $\Omega_{\ell-1}$ (Injection)

Definition of the restriction

A mapping

$$\boldsymbol{F} : \mathbb{R}^{N_\ell} \to \mathbb{R}^{N_{\ell-1}}$$

is called restriction from Ω_ℓ to $\Omega_{\ell-1}$, if it is linear und surjective.

- Graphical presentation:

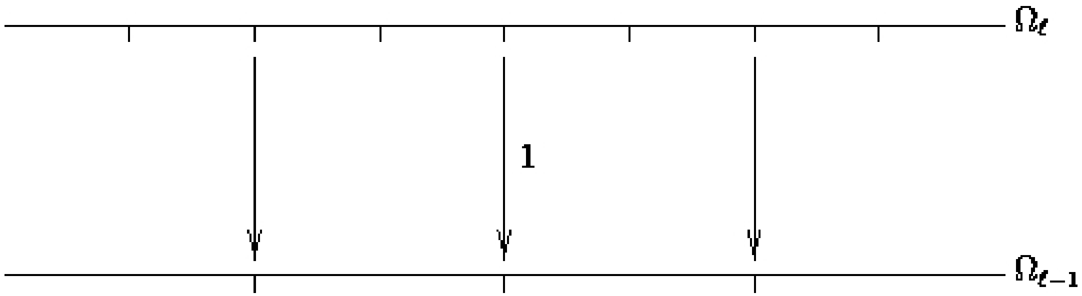

- Matrix representation:

$$\boldsymbol{R}_\ell^{\ell-1} = \begin{pmatrix} 0 & 1 & 0 & & & & \\ & & 0 & 1 & 0 & & \\ & & & \ddots & \ddots & \ddots & \\ & & & & 0 & 1 & 0 \end{pmatrix} \in \mathbb{R}^{N_{\ell-1} \times N_\ell}$$

Mapping from Ω_ℓ to $\Omega_{\ell-1}$ (Linear restriction)

Definition of the restriction

A mapping

$$\boldsymbol{F} : \mathbb{R}^{N_\ell} \to \mathbb{R}^{N_{\ell-1}}$$

is called restriction from Ω_ℓ to $\Omega_{\ell-1}$, if it is linear und surjective.

- Graphical presentation:

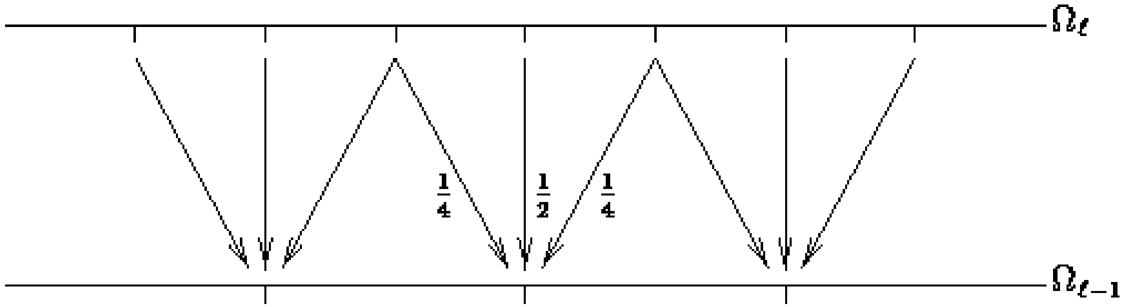

- Matrix representation:

$$\boldsymbol{R}_\ell^{\ell-1} = \frac{1}{4} \begin{pmatrix} 1 & 2 & 1 & & & & \\ & & 1 & 2 & 1 & & \\ & & & \ddots & \ddots & \ddots & \\ & & & & 1 & 2 & 1 \end{pmatrix} \in \mathbb{R}^{N_{\ell-1} \times N_\ell}$$

Effect of the restriction on the Fourier modes

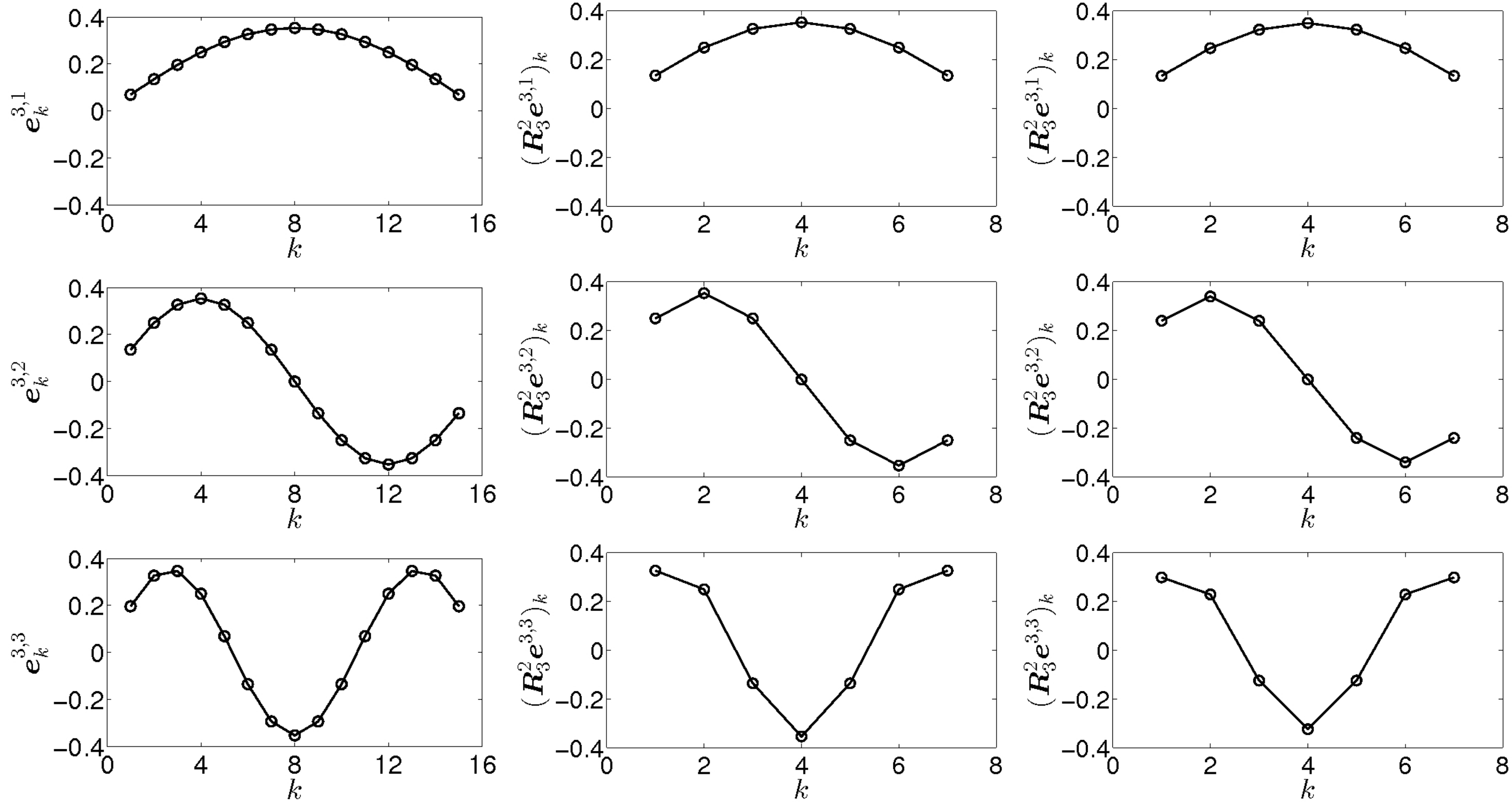

Original

Injection

Linear restriction

Effect of the restriction on the Fourier modes

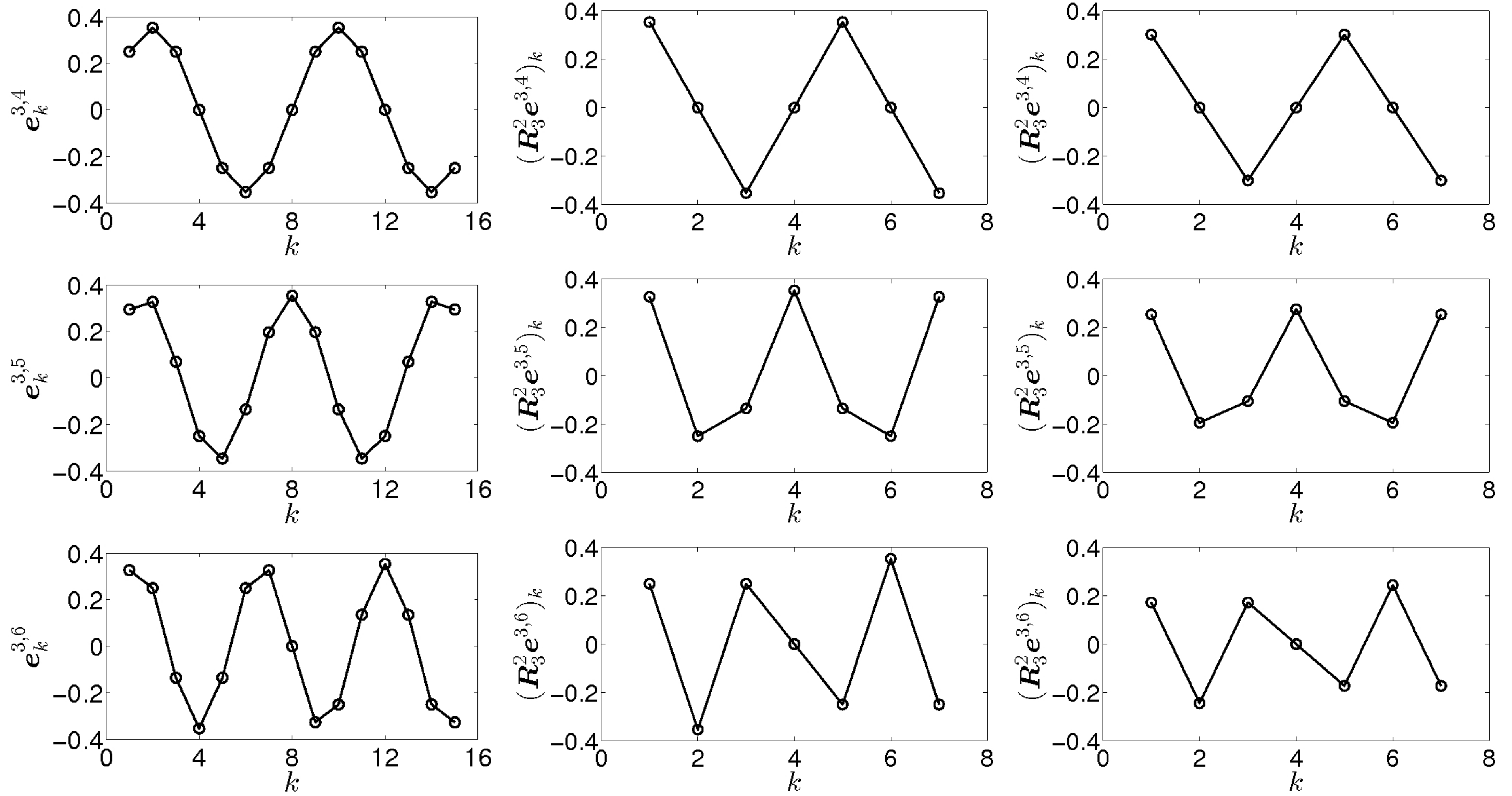

Original Injection Linear restriction

Effect of the restriction on the Fourier modes

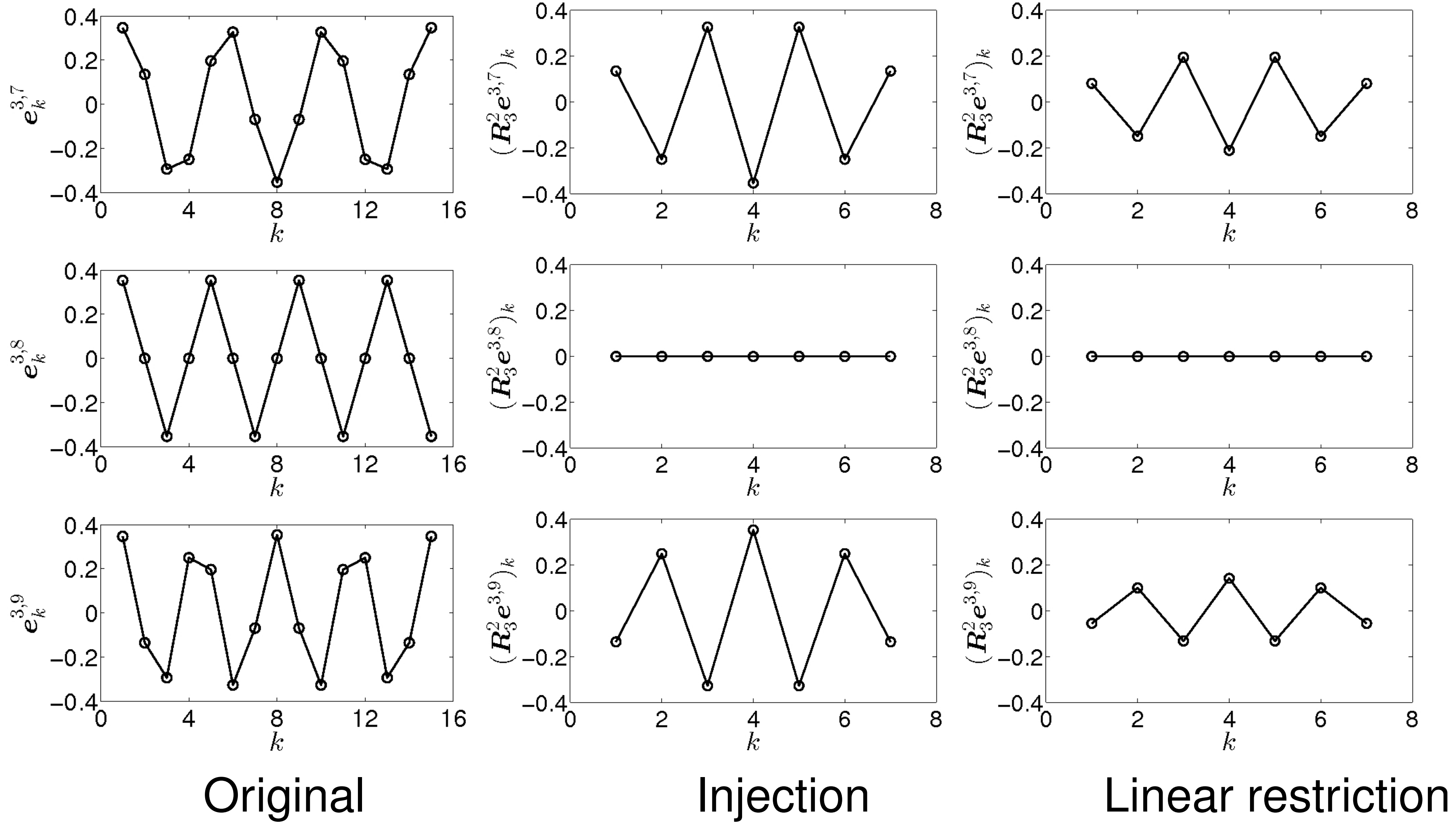

Effect of the restriction on the Fourier modes

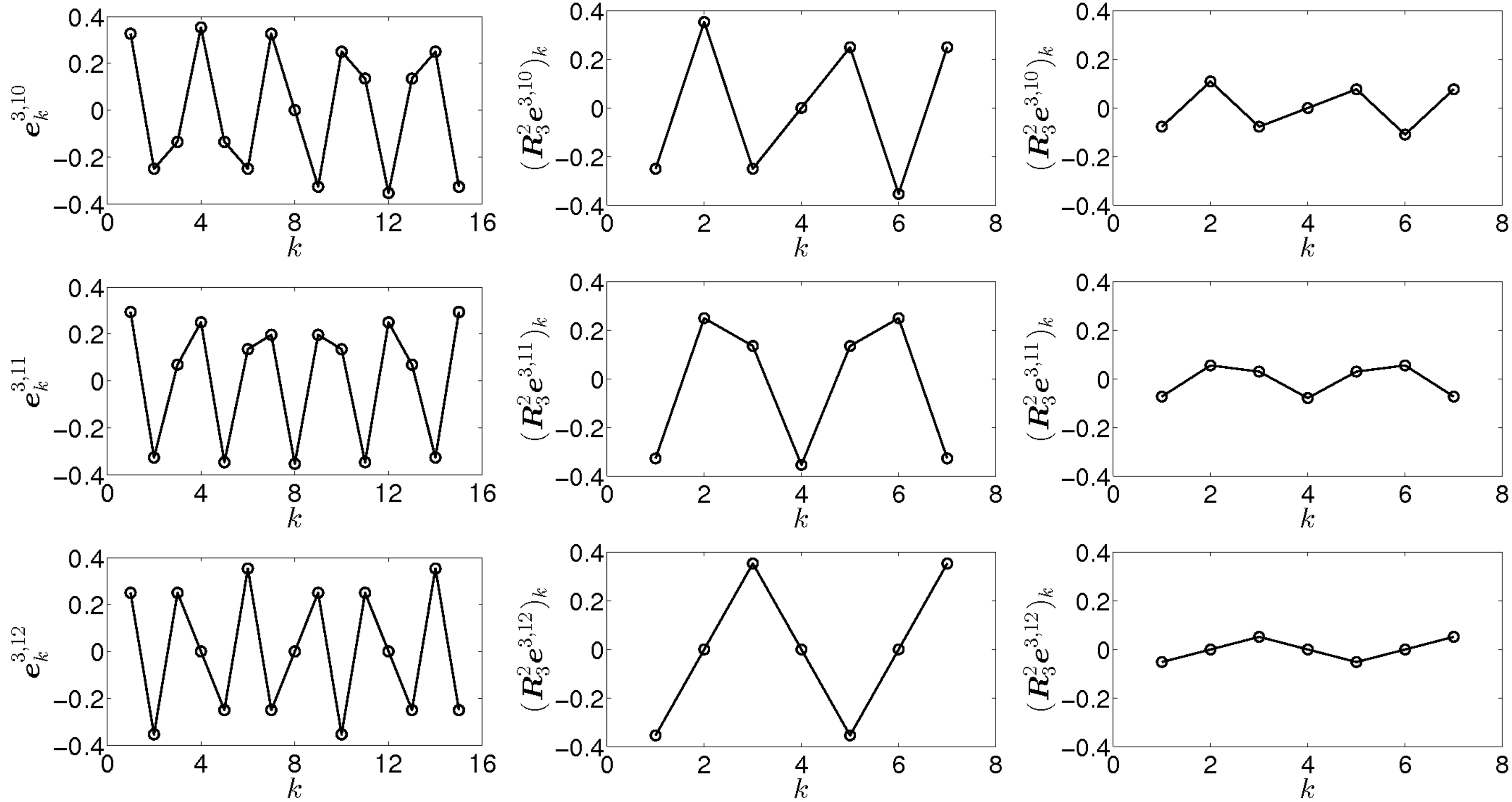

Original Injection Linear restriction

Effect of the restriction on the Fourier modes

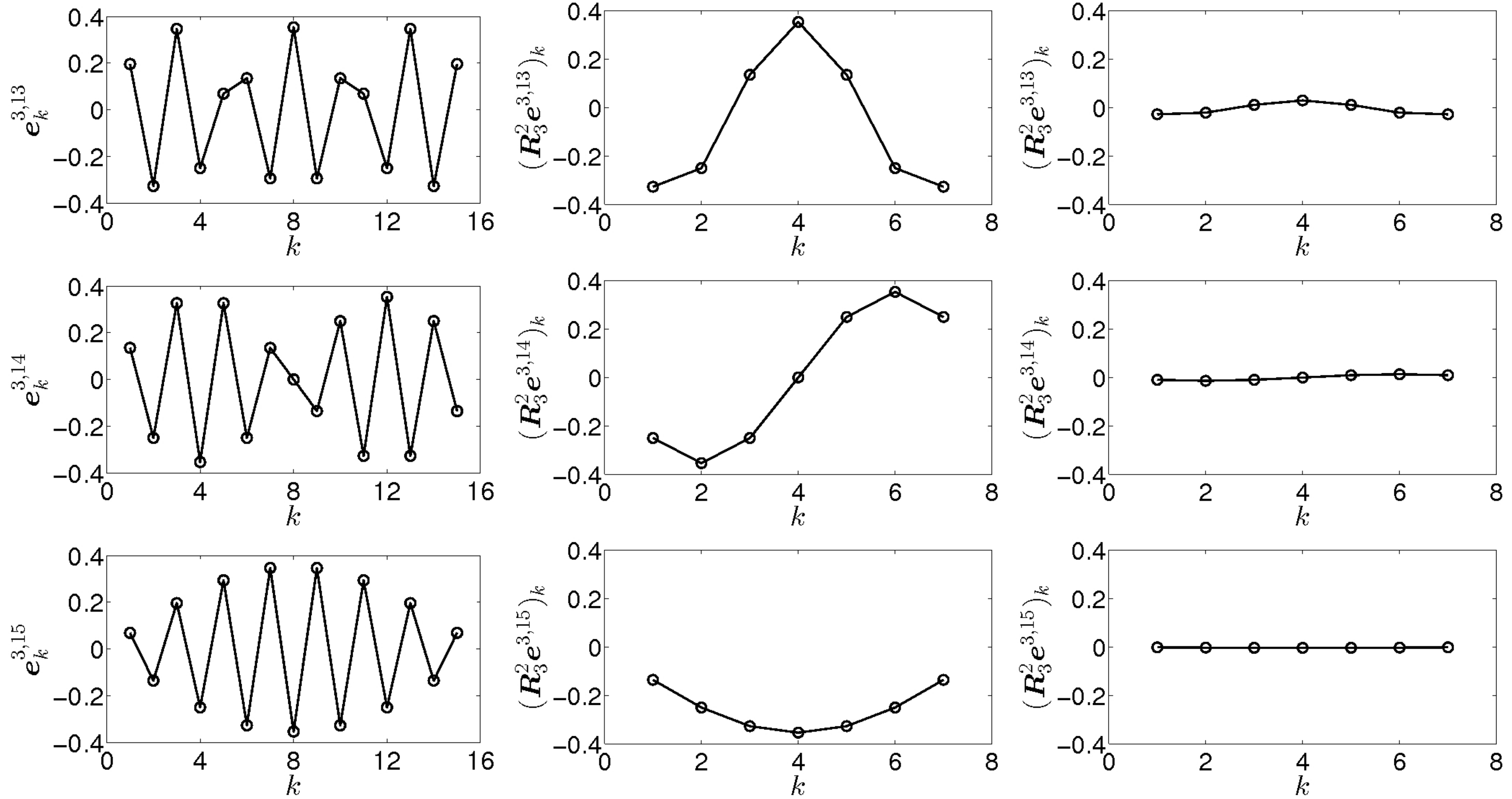

Original Injection Linear restriction

Analysis of the Injection

Theorem

The images of the Fourier modes $\boldsymbol{e}^{\ell,j}$, $j = 1, \ldots, N_\ell$ on Ω_ℓ concerning the **injection** satisfy

$$\boldsymbol{R}_\ell^{\ell-1}\boldsymbol{e}^{\ell,j} = \frac{1}{\sqrt{2}}\boldsymbol{e}^{\ell-1,j} \quad \text{for } j \in \{1, \ldots, N_{\ell-1}\},$$

$$\boldsymbol{R}_\ell^{\ell-1}\boldsymbol{e}^{\ell,j} = \boldsymbol{0} \quad \text{for } j = N_{\ell-1} + 1,$$

$$\boldsymbol{R}_\ell^{\ell-1}\boldsymbol{e}^{\ell,j} = -\frac{1}{\sqrt{2}}\boldsymbol{e}^{\ell-1,\bar{\jmath}} \quad \text{for } j = N_\ell + 1 - \bar{\jmath} \text{ with } \bar{\jmath} \in \{1, \ldots, N_{\ell-1}\}.$$

Theorem

The images of the Fourier modes $\boldsymbol{e}^{\ell,j}$, $j = 1,\ldots,N_\ell$ on Ω_ℓ concerning the **injection** satisfy

$$\begin{aligned}
\boldsymbol{R}_\ell^{\ell-1}\boldsymbol{e}^{\ell,j} &= \frac{1}{\sqrt{2}}\boldsymbol{e}^{\ell-1,j} && \text{for } j \in \{1,\ldots,N_{\ell-1}\},\\
\boldsymbol{R}_\ell^{\ell-1}\boldsymbol{e}^{\ell,j} &= \boldsymbol{0} && \text{for } j = N_{\ell-1}+1,\\
\boldsymbol{R}_\ell^{\ell-1}\boldsymbol{e}^{\ell,j} &= -\frac{1}{\sqrt{2}}\boldsymbol{e}^{\ell-1,\bar{\jmath}} && \text{for } j = N_\ell + 1 - \bar{\jmath} \text{ with } \bar{\jmath} \in \{1,\ldots,N_{\ell-1}\}.
\end{aligned}$$

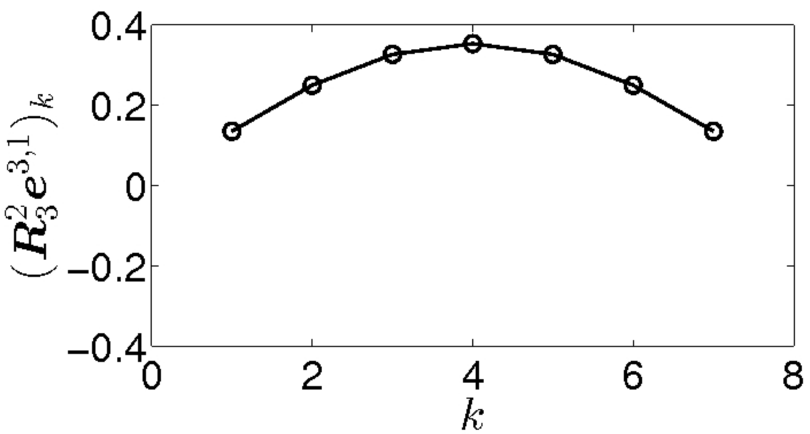

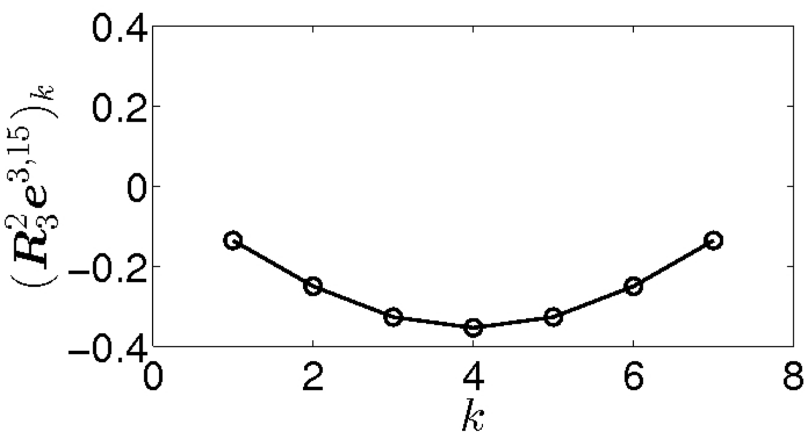

Analysis of the Injection

Theorem

The images of the Fourier modes $\boldsymbol{e}^{\ell,j}$, $j = 1, \ldots, N_\ell$ on Ω_ℓ concerning the **injection** satisfy

$$\begin{aligned}
\boldsymbol{R}_\ell^{\ell-1} \boldsymbol{e}^{\ell,j} &= \frac{1}{\sqrt{2}} \boldsymbol{e}^{\ell-1,j} && \text{for } j \in \{1, \ldots, N_{\ell-1}\}, \\
\boldsymbol{R}_\ell^{\ell-1} \boldsymbol{e}^{\ell,j} &= \boldsymbol{0} && \text{for } j = N_{\ell-1} + 1, \\
\boldsymbol{R}_\ell^{\ell-1} \boldsymbol{e}^{\ell,j} &= -\frac{1}{\sqrt{2}} \boldsymbol{e}^{\ell-1,\bar{\jmath}} && \text{for } j = N_\ell + 1 - \bar{\jmath} \text{ with } \bar{\jmath} \in \{1, \ldots, N_{\ell-1}\}.
\end{aligned}$$

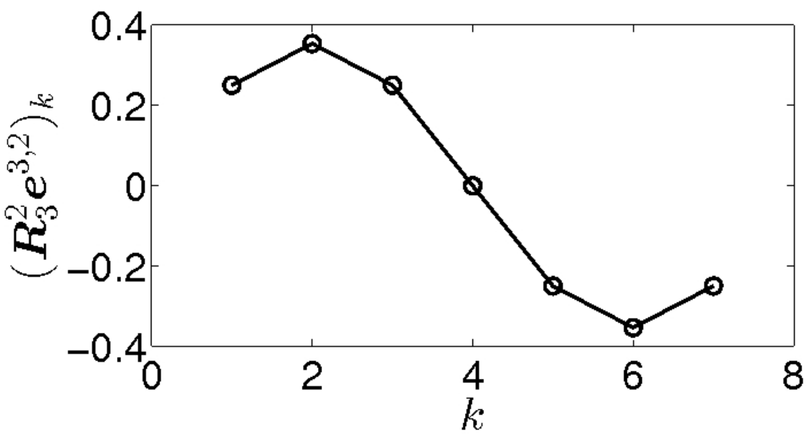

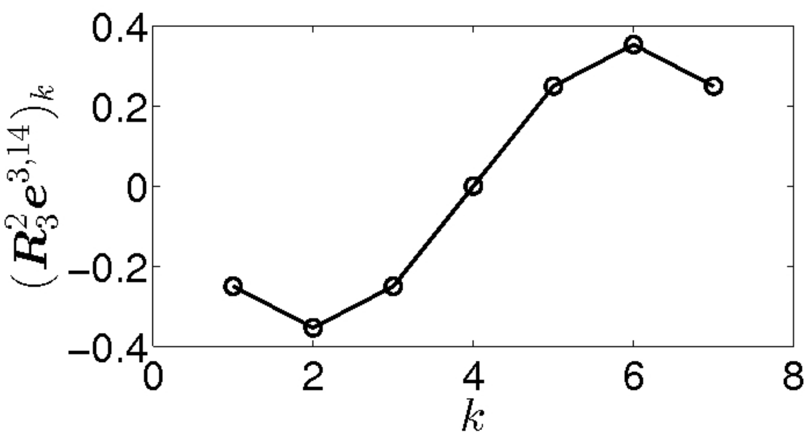

Analysis of the Injection

Theorem

The images of the Fourier modes $\boldsymbol{e}^{\ell,j}$, $j = 1, \ldots, N_\ell$ on Ω_ℓ concerning the **injection** satisfy

$$\boldsymbol{R}_\ell^{\ell-1}\boldsymbol{e}^{\ell,j} = \frac{1}{\sqrt{2}}\boldsymbol{e}^{\ell-1,j} \quad \text{for } j \in \{1, \ldots, N_{\ell-1}\},$$

$$\boldsymbol{R}_\ell^{\ell-1}\boldsymbol{e}^{\ell,j} = \boldsymbol{0} \quad \text{for } j = N_{\ell-1} + 1,$$

$$\boldsymbol{R}_\ell^{\ell-1}\boldsymbol{e}^{\ell,j} = -\frac{1}{\sqrt{2}}\boldsymbol{e}^{\ell-1,\bar{\jmath}} \quad \text{for } j = N_\ell + 1 - \bar{\jmath} \text{ with } \bar{\jmath} \in \{1, \ldots, N_{\ell-1}\}.$$

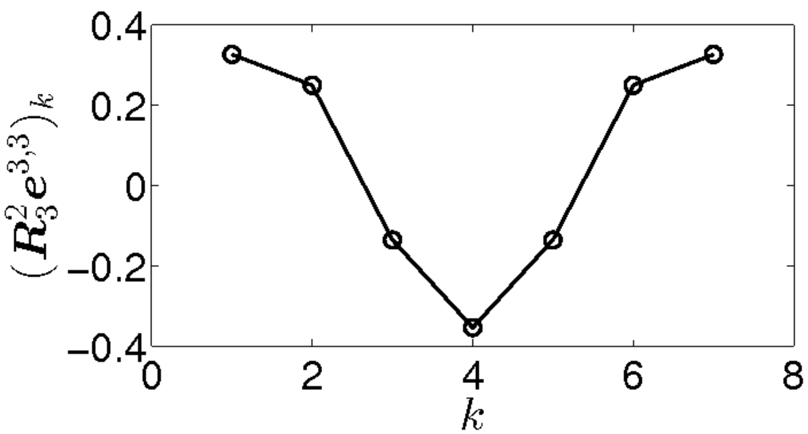

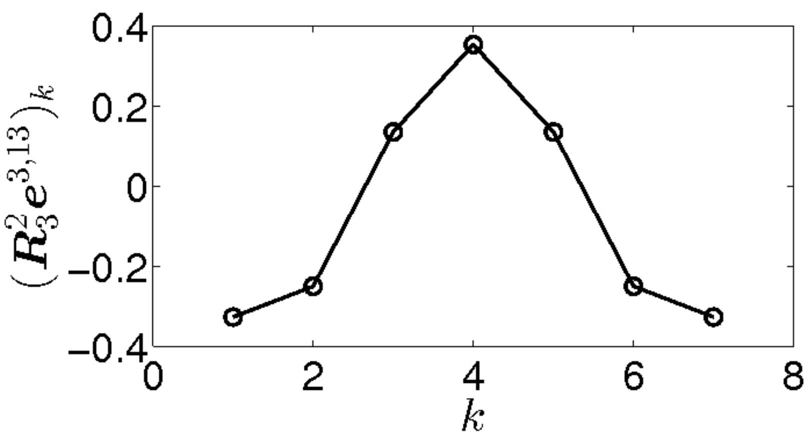

Analysis of the Injection

Theorem

The images of the Fourier modes $\boldsymbol{e}^{\ell,j}$, $j = 1, \ldots, N_\ell$ on Ω_ℓ concerning the **injection** satisfy

$$\boldsymbol{R}_\ell^{\ell-1}\boldsymbol{e}^{\ell,j} = \frac{1}{\sqrt{2}}\boldsymbol{e}^{\ell-1,j} \quad \text{for } j \in \{1, \ldots, N_{\ell-1}\},$$

$$\boldsymbol{R}_\ell^{\ell-1}\boldsymbol{e}^{\ell,j} = \boldsymbol{0} \quad \text{for } j = N_{\ell-1}+1,$$

$$\boldsymbol{R}_\ell^{\ell-1}\boldsymbol{e}^{\ell,j} = -\frac{1}{\sqrt{2}}\boldsymbol{e}^{\ell-1,\bar{\jmath}} \quad \text{for } j = N_\ell + 1 - \bar{\jmath} \text{ with } \bar{\jmath} \in \{1, \ldots, N_{\ell-1}\}.$$

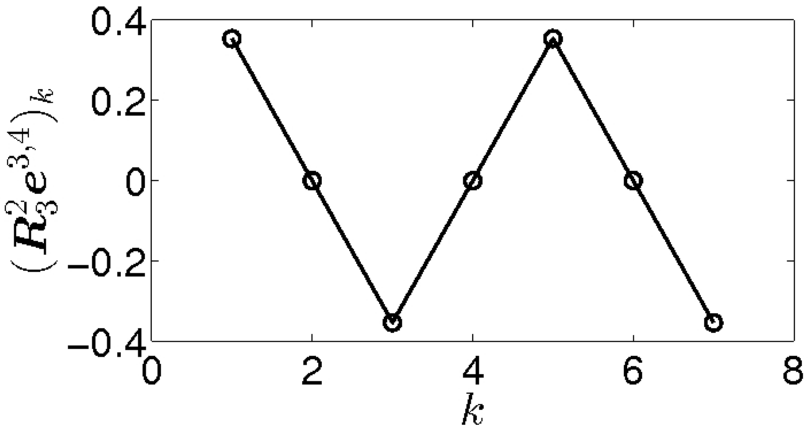

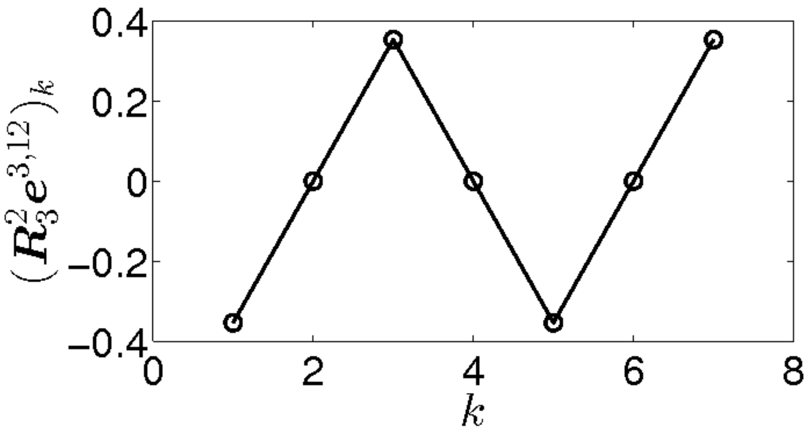

Analysis of the Injection

Theorem

The images of the Fourier modes $\boldsymbol{e}^{\ell,j}$, $j = 1, \ldots, N_\ell$ on Ω_ℓ concerning the **injection** satisfy

$$\boldsymbol{R}_\ell^{\ell-1}\boldsymbol{e}^{\ell,j} = \frac{1}{\sqrt{2}}\boldsymbol{e}^{\ell-1,j} \quad \text{for } j \in \{1, \ldots, N_{\ell-1}\},$$

$$\boldsymbol{R}_\ell^{\ell-1}\boldsymbol{e}^{\ell,j} = \boldsymbol{0} \quad \text{for } j = N_{\ell-1} + 1,$$

$$\boldsymbol{R}_\ell^{\ell-1}\boldsymbol{e}^{\ell,j} = -\frac{1}{\sqrt{2}}\boldsymbol{e}^{\ell-1,\bar{\jmath}} \quad \text{for } j = N_\ell + 1 - \bar{\jmath} \text{ with } \bar{\jmath} \in \{1, \ldots, N_{\ell-1}\}.$$

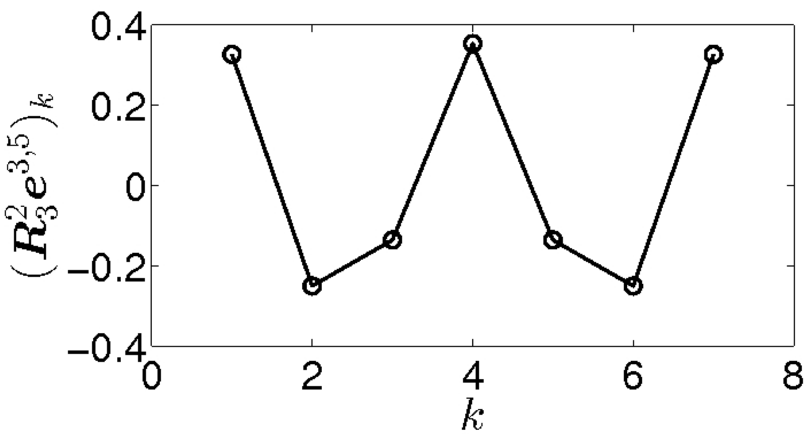

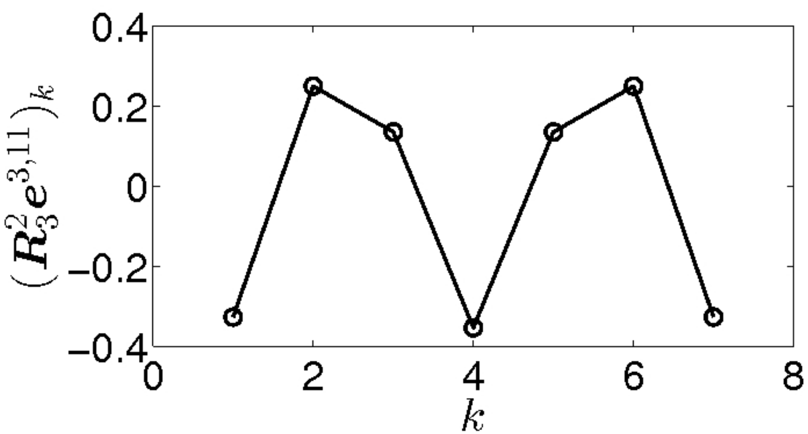

Analysis of the Injection

Theorem

The images of the Fourier modes $\boldsymbol{e}^{\ell,j}$, $j = 1, \ldots, N_\ell$ on Ω_ℓ concerning the **injection** satisfy

$$\begin{aligned}
\boldsymbol{R}_\ell^{\ell-1}\boldsymbol{e}^{\ell,j} &= \frac{1}{\sqrt{2}}\boldsymbol{e}^{\ell-1,j} && \text{for } j \in \{1, \ldots, N_{\ell-1}\}, \\
\boldsymbol{R}_\ell^{\ell-1}\boldsymbol{e}^{\ell,j} &= \boldsymbol{0} && \text{for } j = N_{\ell-1} + 1, \\
\boldsymbol{R}_\ell^{\ell-1}\boldsymbol{e}^{\ell,j} &= -\frac{1}{\sqrt{2}}\boldsymbol{e}^{\ell-1,\bar{\jmath}} && \text{for } j = N_\ell + 1 - \bar{\jmath} \text{ with } \bar{\jmath} \in \{1, \ldots, N_{\ell-1}\}.
\end{aligned}$$

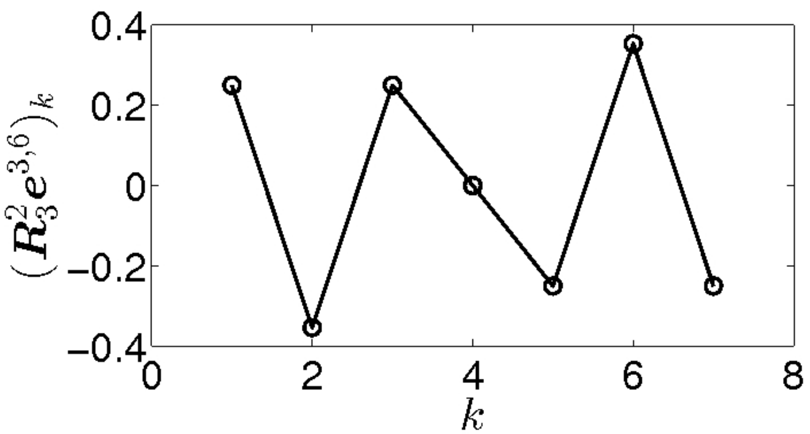

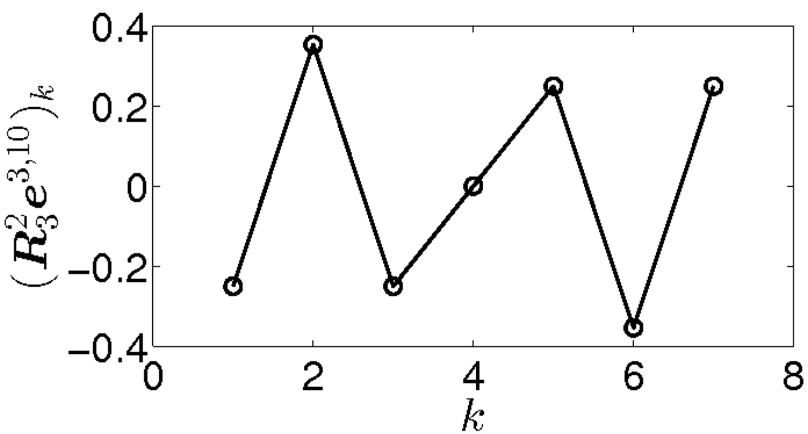

Theorem

The images of the Fourier modes $\boldsymbol{e}^{\ell,j}$, $j = 1, \ldots, N_\ell$ on Ω_ℓ concerning the **injection** satisfy

$$\boldsymbol{R}_\ell^{\ell-1}\boldsymbol{e}^{\ell,j} = \frac{1}{\sqrt{2}}\boldsymbol{e}^{\ell-1,j} \quad \text{for } j \in \{1,\ldots,N_{\ell-1}\},$$

$$\boldsymbol{R}_\ell^{\ell-1}\boldsymbol{e}^{\ell,j} = \mathbf{0} \quad \text{for } j = N_{\ell-1}+1,$$

$$\boldsymbol{R}_\ell^{\ell-1}\boldsymbol{e}^{\ell,j} = -\frac{1}{\sqrt{2}}\boldsymbol{e}^{\ell-1,\bar{\jmath}} \quad \text{for } j = N_\ell + 1 - \bar{\jmath} \text{ with } \bar{\jmath} \in \{1,\ldots,N_{\ell-1}\}.$$

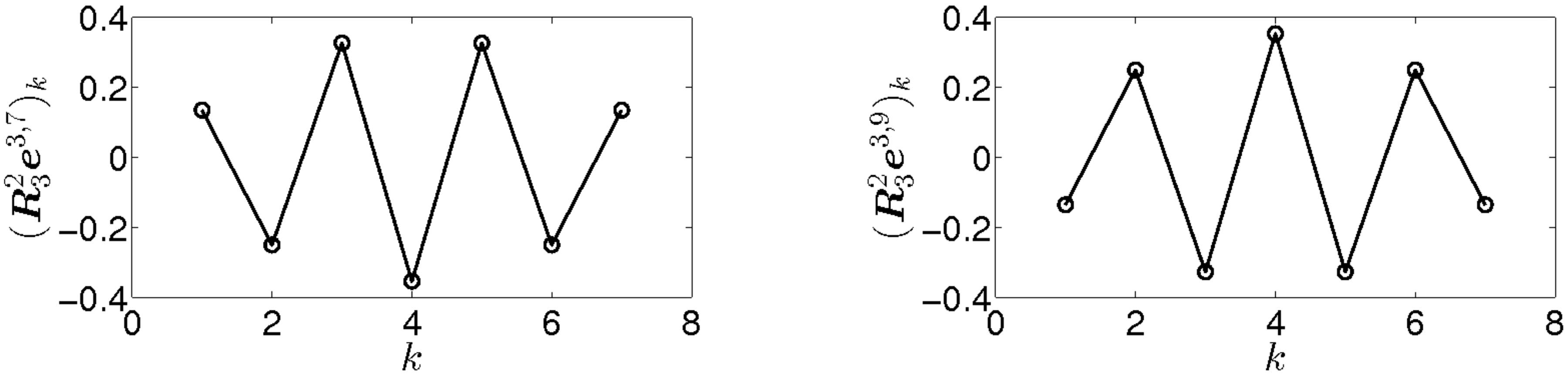

Analysis of the Linear Restriction

Theorem

The images of the Fourier modes $\boldsymbol{e}^{\ell,j}$, $j = 1, \ldots, N_\ell$ on Ω_ℓ concerning the **linear restriction** satisfy

$$\boldsymbol{R}_\ell^{\ell-1}\boldsymbol{e}^{\ell,j} = \frac{c_j}{\sqrt{2}}\boldsymbol{e}^{\ell-1,j} \quad \text{for } j \in \{1, \ldots, N_{\ell-1}\},$$

$$\boldsymbol{R}_\ell^{\ell-1}\boldsymbol{e}^{\ell,j} = \boldsymbol{0} \quad \text{for } j = N_{\ell-1} + 1,$$

$$\boldsymbol{R}_\ell^{\ell-1}\boldsymbol{e}^{\ell,j} = -\frac{s_{\bar{\jmath}}}{\sqrt{2}}\boldsymbol{e}^{\ell-1,\bar{\jmath}} \quad \text{for } j = N_\ell + 1 - \bar{\jmath} \text{ with } \bar{\jmath} \in \{1, \ldots, N_{\ell-1}\}.$$

with $c_j = \cos^2\left(j\pi\frac{h_\ell}{2}\right)$ and $s_{\bar{\jmath}} = \sin^2\left(\bar{\jmath}\pi\frac{h_\ell}{2}\right)$.

Analysis of the Linear Restriction

Theorem

The images of the Fourier modes $\boldsymbol{e}^{\ell,j}$, $j = 1, \ldots, N_\ell$ on Ω_ℓ concerning the **linear restriction** satisfy

$$\boldsymbol{R}_\ell^{\ell-1}\boldsymbol{e}^{\ell,j} = \frac{c_j}{\sqrt{2}}\boldsymbol{e}^{\ell-1,j} \quad \text{for } j \in \{1, \ldots, N_{\ell-1}\},$$

$$\boldsymbol{R}_\ell^{\ell-1}\boldsymbol{e}^{\ell,j} = \boldsymbol{0} \quad \text{for } j = N_{\ell-1}+1,$$

$$\boldsymbol{R}_\ell^{\ell-1}\boldsymbol{e}^{\ell,j} = -\frac{s_{\bar{\jmath}}}{\sqrt{2}}\boldsymbol{e}^{\ell-1,\bar{\jmath}} \quad \text{for } j = N_\ell + 1 - \bar{\jmath} \text{ with } \bar{\jmath} \in \{1, \ldots, N_{\ell-1}\}.$$

with $c_j = \cos^2\left(j\pi\frac{h_\ell}{2}\right)$ and $s_{\bar{\jmath}} = \sin^2\left(\bar{\jmath}\pi\frac{h_\ell}{2}\right)$.

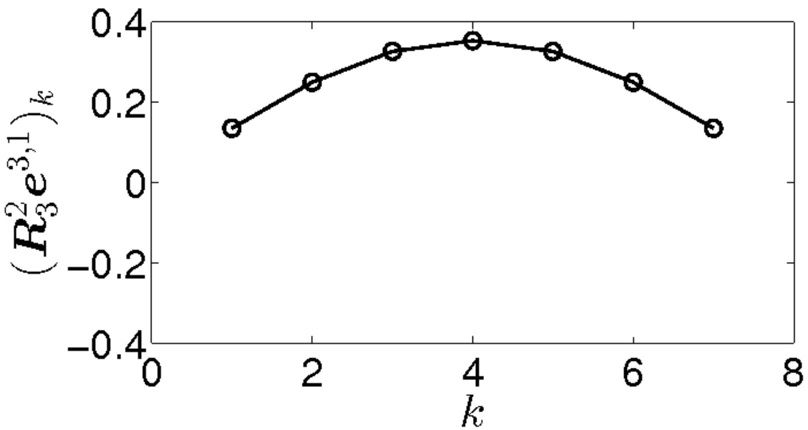

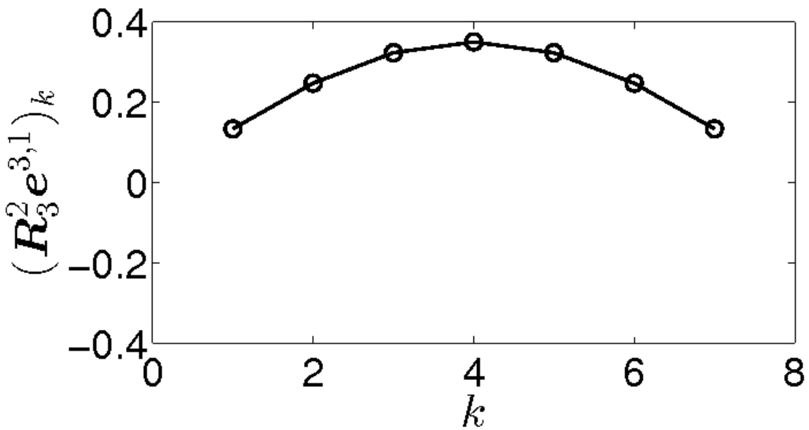

Analysis of the Linear Restriction

Theorem

The images of the Fourier modes $\boldsymbol{e}^{\ell,j}$, $j = 1, \ldots, N_\ell$ on Ω_ℓ concerning the **linear restriction** satisfy

$$\boldsymbol{R}_\ell^{\ell-1}\boldsymbol{e}^{\ell,j} = \frac{c_j}{\sqrt{2}}\boldsymbol{e}^{\ell-1,j} \quad \text{for } j \in \{1, \ldots, N_{\ell-1}\},$$

$$\boldsymbol{R}_\ell^{\ell-1}\boldsymbol{e}^{\ell,j} = \boldsymbol{0} \quad \text{for } j = N_{\ell-1} + 1,$$

$$\boldsymbol{R}_\ell^{\ell-1}\boldsymbol{e}^{\ell,j} = -\frac{s_{\bar{\jmath}}}{\sqrt{2}}\boldsymbol{e}^{\ell-1,\bar{\jmath}} \quad \text{for } j = N_\ell + 1 - \bar{\jmath} \text{ with } \bar{\jmath} \in \{1, \ldots, N_{\ell-1}\}.$$

with $c_j = \cos^2\left(j\pi\frac{h_\ell}{2}\right)$ and $s_{\bar{\jmath}} = \sin^2\left(\bar{\jmath}\pi\frac{h_\ell}{2}\right)$.

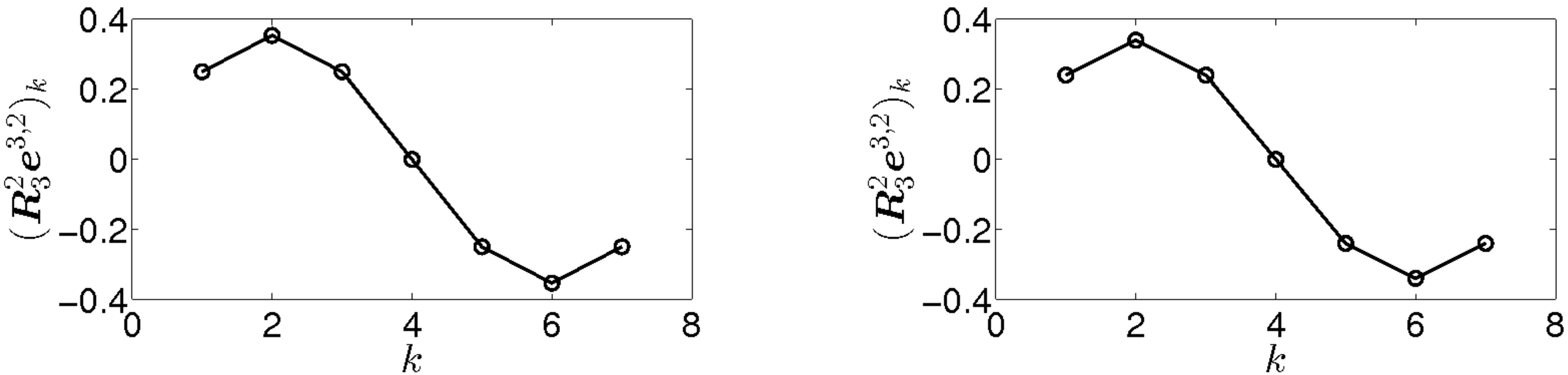

Analysis of the Linear Restriction

Theorem

The images of the Fourier modes $\boldsymbol{e}^{\ell,j}$, $j = 1, \ldots, N_\ell$ on Ω_ℓ concerning the **linear restriction** satisfy

$$\boldsymbol{R}_\ell^{\ell-1}\boldsymbol{e}^{\ell,j} = \frac{c_j}{\sqrt{2}}\boldsymbol{e}^{\ell-1,j} \quad \text{for } j \in \{1, \ldots, N_{\ell-1}\},$$

$$\boldsymbol{R}_\ell^{\ell-1}\boldsymbol{e}^{\ell,j} = \boldsymbol{0} \quad \text{for } j = N_{\ell-1} + 1,$$

$$\boldsymbol{R}_\ell^{\ell-1}\boldsymbol{e}^{\ell,j} = -\frac{s_{\bar{\jmath}}}{\sqrt{2}}\boldsymbol{e}^{\ell-1,\bar{\jmath}} \quad \text{for } j = N_\ell + 1 - \bar{\jmath} \text{ with } \bar{\jmath} \in \{1, \ldots, N_{\ell-1}\}.$$

with $c_j = \cos^2\left(j\pi\frac{h_\ell}{2}\right)$ and $s_{\bar{\jmath}} = \sin^2\left(\bar{\jmath}\pi\frac{h_\ell}{2}\right)$.

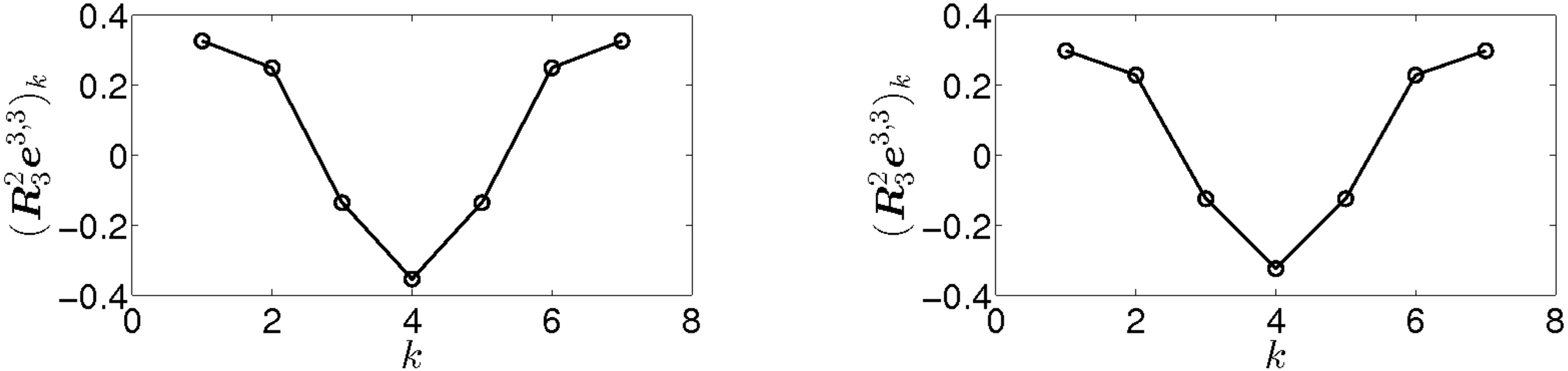

Analysis of the Linear Restriction

Theorem

The images of the Fourier modes $\boldsymbol{e}^{\ell,j}$, $j = 1, \ldots, N_\ell$ on Ω_ℓ concerning the **linear restriction** satisfy

$$\boldsymbol{R}_\ell^{\ell-1}\boldsymbol{e}^{\ell,j} = \frac{c_j}{\sqrt{2}}\boldsymbol{e}^{\ell-1,j} \quad \text{for } j \in \{1, \ldots, N_{\ell-1}\},$$

$$\boldsymbol{R}_\ell^{\ell-1}\boldsymbol{e}^{\ell,j} = \boldsymbol{0} \quad \text{for } j = N_{\ell-1} + 1,$$

$$\boldsymbol{R}_\ell^{\ell-1}\boldsymbol{e}^{\ell,j} = -\frac{s_{\bar{\jmath}}}{\sqrt{2}}\boldsymbol{e}^{\ell-1,\bar{\jmath}} \quad \text{for } j = N_\ell + 1 - \bar{\jmath} \text{ with } \bar{\jmath} \in \{1, \ldots, N_{\ell-1}\}.$$

with $c_j = \cos^2\left(j\pi\frac{h_\ell}{2}\right)$ and $s_{\bar{\jmath}} = \sin^2\left(\bar{\jmath}\pi\frac{h_\ell}{2}\right)$.

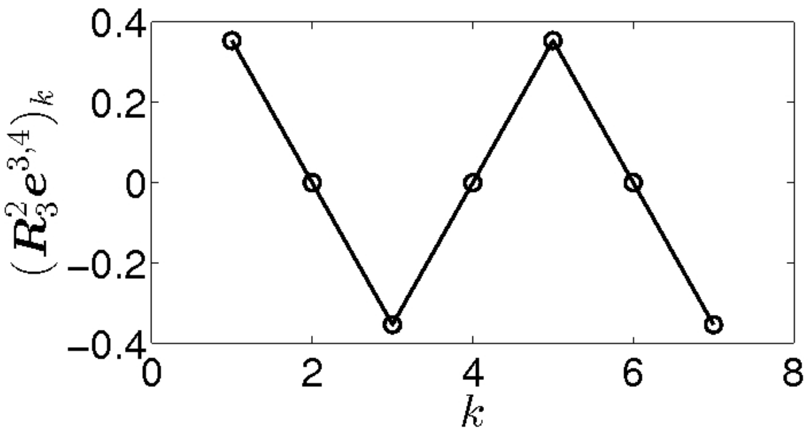

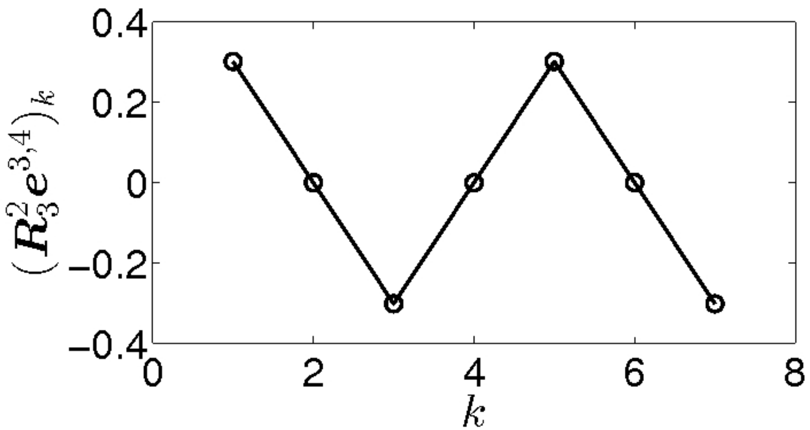

Analysis of the Linear Restriction

Theorem

The images of the Fourier modes $\boldsymbol{e}^{\ell,j}$, $j = 1,\dots,N_\ell$ on Ω_ℓ concerning the **linear restriction** satisfy

$$\begin{aligned}
\boldsymbol{R}_\ell^{\ell-1}\boldsymbol{e}^{\ell,j} &= \frac{c_j}{\sqrt{2}}\boldsymbol{e}^{\ell-1,j} && \text{for } j \in \{1,\dots,N_{\ell-1}\},\\
\boldsymbol{R}_\ell^{\ell-1}\boldsymbol{e}^{\ell,j} &= \boldsymbol{0} && \text{for } j = N_{\ell-1}+1,\\
\boldsymbol{R}_\ell^{\ell-1}\boldsymbol{e}^{\ell,j} &= -\frac{s_{\bar{\jmath}}}{\sqrt{2}}\boldsymbol{e}^{\ell-1,\bar{\jmath}} && \text{for } j = N_\ell + 1 - \bar{\jmath} \text{ with } \bar{\jmath} \in \{1,\dots,N_{\ell-1}\}.
\end{aligned}$$

with $c_j = \cos^2\left(j\pi\frac{h_\ell}{2}\right)$ and $s_{\bar{\jmath}} = \sin^2\left(\bar{\jmath}\pi\frac{h_\ell}{2}\right)$.

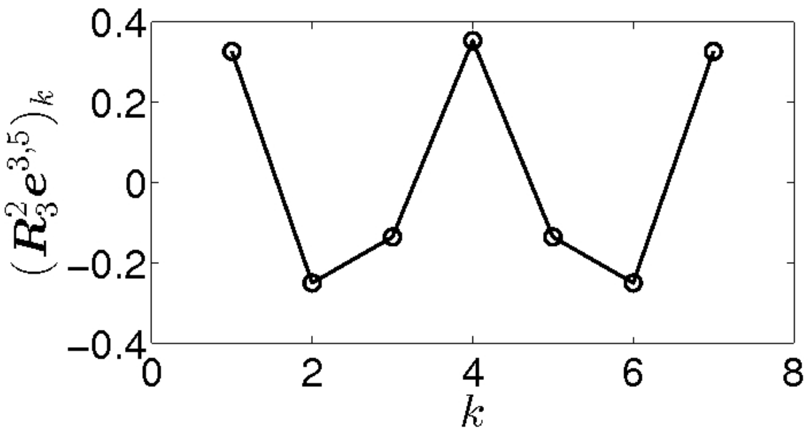

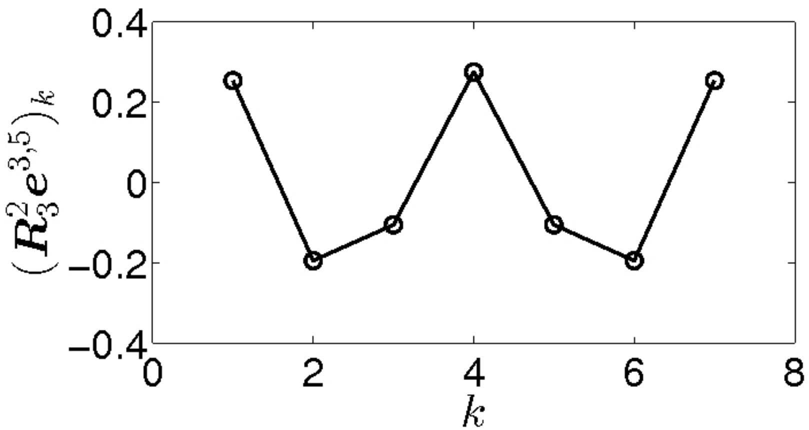

Analysis of the Linear Restriction

Theorem

The images of the Fourier modes $\boldsymbol{e}^{\ell,j}$, $j = 1, \ldots, N_\ell$ on Ω_ℓ concerning the **linear restriction** satisfy

$$\begin{aligned}
\boldsymbol{R}_\ell^{\ell-1}\boldsymbol{e}^{\ell,j} &= \frac{c_j}{\sqrt{2}}\boldsymbol{e}^{\ell-1,j} && \text{for } j \in \{1, \ldots, N_{\ell-1}\}, \\
\boldsymbol{R}_\ell^{\ell-1}\boldsymbol{e}^{\ell,j} &= \boldsymbol{0} && \text{for } j = N_{\ell-1} + 1, \\
\boldsymbol{R}_\ell^{\ell-1}\boldsymbol{e}^{\ell,j} &= -\frac{s_{\bar{\jmath}}}{\sqrt{2}}\boldsymbol{e}^{\ell-1,\bar{\jmath}} && \text{for } j = N_\ell + 1 - \bar{\jmath} \text{ with } \bar{\jmath} \in \{1, \ldots, N_{\ell-1}\}.
\end{aligned}$$

with $c_j = \cos^2\left(j\pi\frac{h_\ell}{2}\right)$ and $s_{\bar{\jmath}} = \sin^2\left(\bar{\jmath}\pi\frac{h_\ell}{2}\right)$.

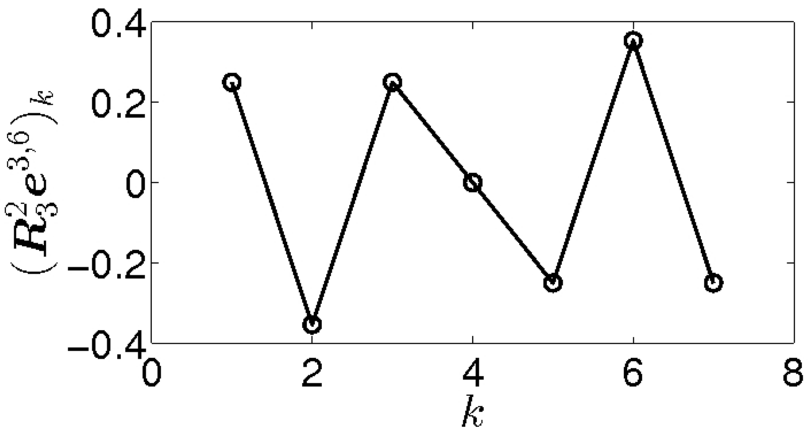

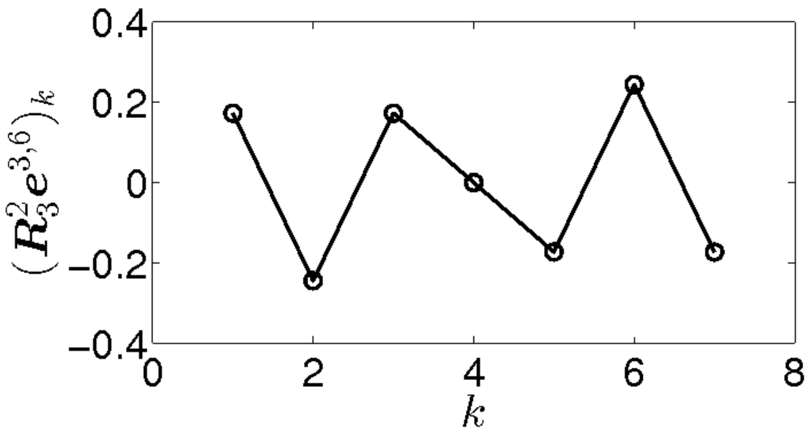

Analysis of the Linear Restriction

Theorem

The images of the Fourier modes $\boldsymbol{e}^{\ell,j}$, $j = 1, \ldots, N_\ell$ on Ω_ℓ concerning the **linear restriction** satisfy

$$\boldsymbol{R}_\ell^{\ell-1} \mathbf{e}^{\ell,j} = \frac{c_j}{\sqrt{2}} \mathbf{e}^{\ell-1,j} \quad \text{for } j \in \{1, \ldots, N_{\ell-1}\},$$

$$\boldsymbol{R}_\ell^{\ell-1} \mathbf{e}^{\ell,j} = \mathbf{0} \quad \text{for } j = N_{\ell-1} + 1,$$

$$\boldsymbol{R}_\ell^{\ell-1} \mathbf{e}^{\ell,j} = -\frac{s_{\bar{\jmath}}}{\sqrt{2}} \mathbf{e}^{\ell-1,\bar{\jmath}} \quad \text{for } j = N_\ell + 1 - \bar{\jmath} \text{ with } \bar{\jmath} \in \{1, \ldots, N_{\ell-1}\}.$$

with $c_j = \cos^2\left(j\pi \frac{h_\ell}{2}\right)$ and $s_{\bar{\jmath}} = \sin^2\left(\bar{\jmath}\pi \frac{h_\ell}{2}\right)$.

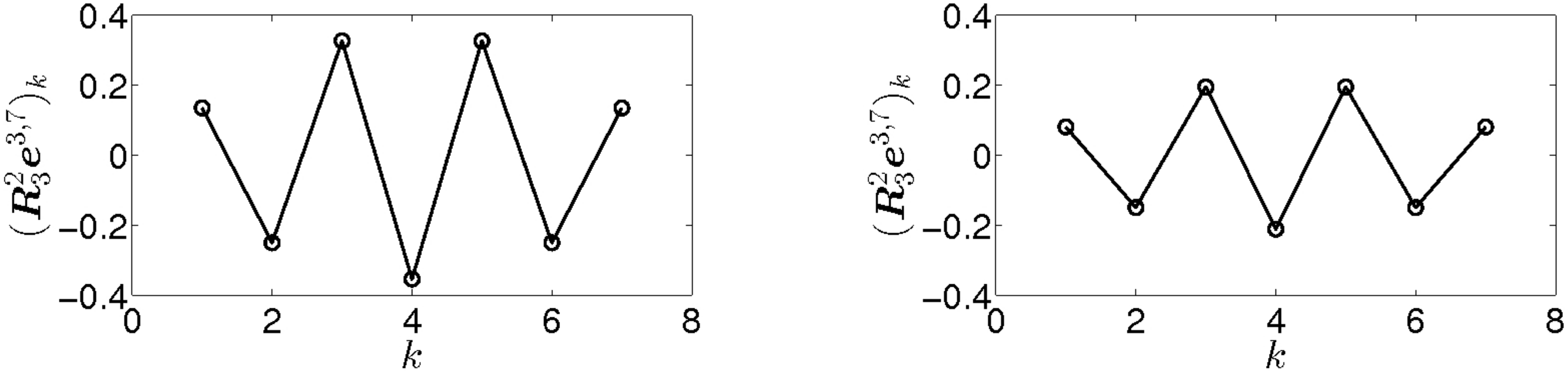

Analysis of the Linear Restriction

Theorem

The images of the Fourier modes $\boldsymbol{e}^{\ell,j}$, $j = 1, \ldots, N_\ell$ on Ω_ℓ concerning the **linear restriction** satisfy

$$\boldsymbol{R}_\ell^{\ell-1}\boldsymbol{e}^{\ell,j} = \frac{c_j}{\sqrt{2}}\boldsymbol{e}^{\ell-1,j} \quad \text{for } j \in \{1, \ldots, N_{\ell-1}\},$$

$$\boldsymbol{R}_\ell^{\ell-1}\boldsymbol{e}^{\ell,j} = \boldsymbol{0} \quad \text{for } j = N_{\ell-1} + 1,$$

$$\boldsymbol{R}_\ell^{\ell-1}\boldsymbol{e}^{\ell,j} = -\frac{s_{\bar{\jmath}}}{\sqrt{2}}\boldsymbol{e}^{\ell-1,\bar{\jmath}} \quad \text{for } j = N_\ell + 1 - \bar{\jmath} \text{ with } \bar{\jmath} \in \{1, \ldots, N_{\ell-1}\}.$$

with $c_j = \cos^2\left(j\pi\frac{h_\ell}{2}\right)$ and $s_{\bar{\jmath}} = \sin^2\left(\bar{\jmath}\pi\frac{h_\ell}{2}\right)$.

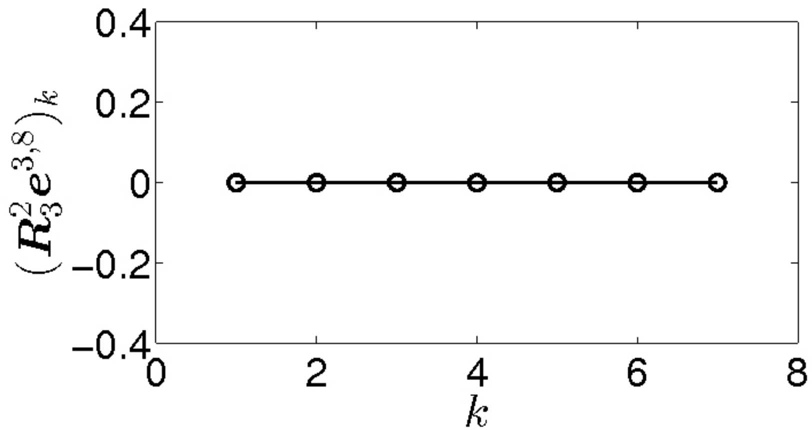

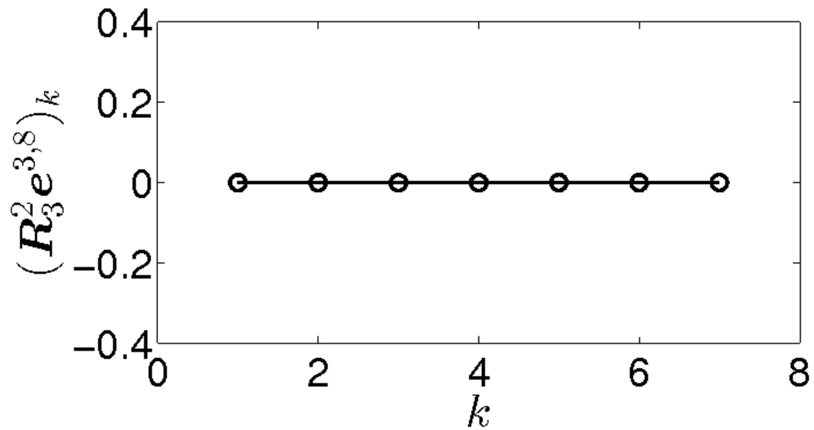

Analysis of the Linear Restriction

Theorem

The images of the Fourier modes $\boldsymbol{e}^{\ell,j}$, $j = 1, \ldots, N_\ell$ on Ω_ℓ concerning the **linear restriction** satisfy

$$\boldsymbol{R}_\ell^{\ell-1}\boldsymbol{e}^{\ell,j} = \frac{c_j}{\sqrt{2}}\boldsymbol{e}^{\ell-1,j} \quad \text{for } j \in \{1, \ldots, N_{\ell-1}\},$$

$$\boldsymbol{R}_\ell^{\ell-1}\boldsymbol{e}^{\ell,j} = \mathbf{0} \quad \text{for } j = N_{\ell-1} + 1,$$

$$\boldsymbol{R}_\ell^{\ell-1}\boldsymbol{e}^{\ell,j} = -\frac{s_{\bar{\jmath}}}{\sqrt{2}}\boldsymbol{e}^{\ell-1,\bar{\jmath}} \quad \text{for } j = N_\ell + 1 - \bar{\jmath} \text{ with } \bar{\jmath} \in \{1, \ldots, N_{\ell-1}\}.$$

with $c_j = \cos^2\left(j\pi\frac{h_\ell}{2}\right)$ and $s_{\bar{\jmath}} = \sin^2\left(\bar{\jmath}\pi\frac{h_\ell}{2}\right)$.

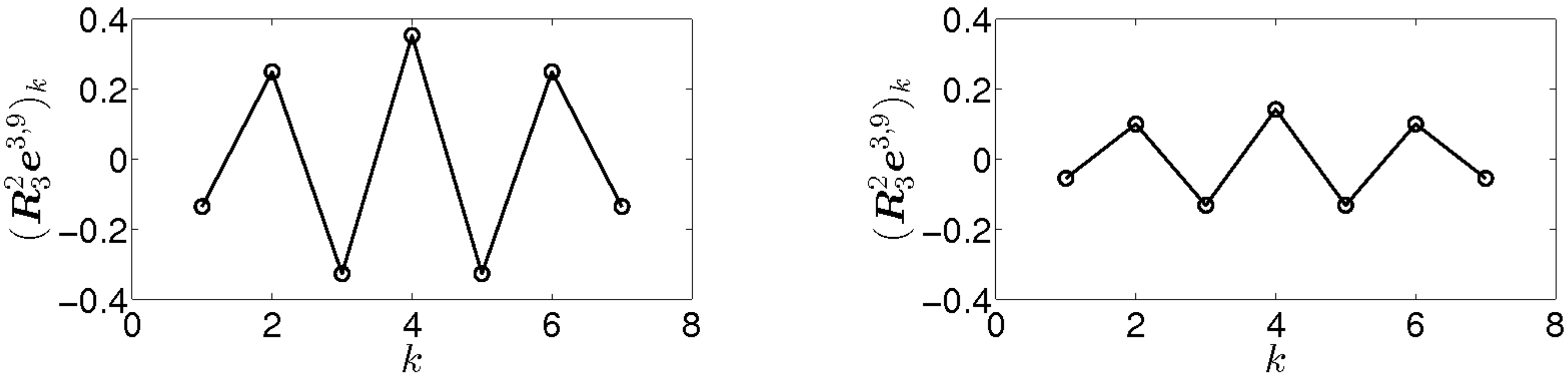

Analysis of the Linear Restriction

Theorem

The images of the Fourier modes $\boldsymbol{e}^{\ell,j}$, $j = 1, \ldots, N_\ell$ on Ω_ℓ concerning the **linear restriction** satisfy

$$\boldsymbol{R}_\ell^{\ell-1}\boldsymbol{e}^{\ell,j} = \frac{c_j}{\sqrt{2}}\boldsymbol{e}^{\ell-1,j} \quad \text{for } j \in \{1, \ldots, N_{\ell-1}\},$$

$$\boldsymbol{R}_\ell^{\ell-1}\boldsymbol{e}^{\ell,j} = \boldsymbol{0} \quad \text{for } j = N_{\ell-1} + 1,$$

$$\boldsymbol{R}_\ell^{\ell-1}\boldsymbol{e}^{\ell,j} = -\frac{s_{\bar{\jmath}}}{\sqrt{2}}\boldsymbol{e}^{\ell-1,\bar{\jmath}} \quad \text{for } j = N_\ell + 1 - \bar{\jmath} \text{ with } \bar{\jmath} \in \{1, \ldots, N_{\ell-1}\}.$$

with $c_j = \cos^2\left(j\pi\frac{h_\ell}{2}\right)$ and $s_{\bar{\jmath}} = \sin^2\left(\bar{\jmath}\pi\frac{h_\ell}{2}\right)$.

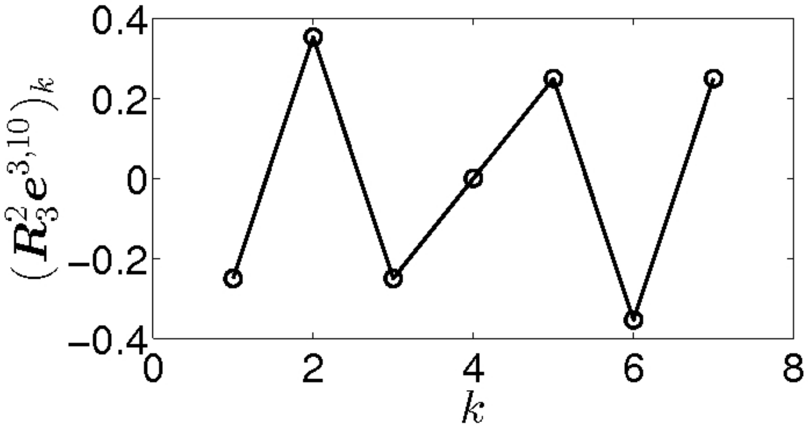

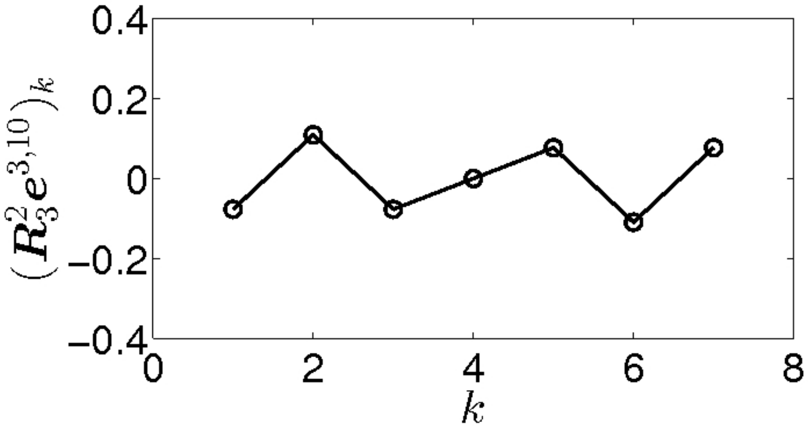

Analysis of the Linear Restriction

Theorem

The images of the Fourier modes $\boldsymbol{e}^{\ell,j}$, $j = 1, \dots, N_\ell$ on Ω_ℓ concerning the **linear restriction** satisfy

$$\boldsymbol{R}_\ell^{\ell-1}\boldsymbol{e}^{\ell,j} = \frac{c_j}{\sqrt{2}}\boldsymbol{e}^{\ell-1,j} \quad \text{for } j \in \{1,\dots,N_{\ell-1}\},$$

$$\boldsymbol{R}_\ell^{\ell-1}\boldsymbol{e}^{\ell,j} = \boldsymbol{0} \quad \text{for } j = N_{\ell-1}+1,$$

$$\boldsymbol{R}_\ell^{\ell-1}\boldsymbol{e}^{\ell,j} = -\frac{s_{\bar{\jmath}}}{\sqrt{2}}\boldsymbol{e}^{\ell-1,\bar{\jmath}} \quad \text{for } j = N_\ell + 1 - \bar{\jmath} \text{ with } \bar{\jmath} \in \{1,\dots,N_{\ell-1}\}.$$

with $c_j = \cos^2\left(j\pi\frac{h_\ell}{2}\right)$ and $s_{\bar{\jmath}} = \sin^2\left(\bar{\jmath}\pi\frac{h_\ell}{2}\right)$.

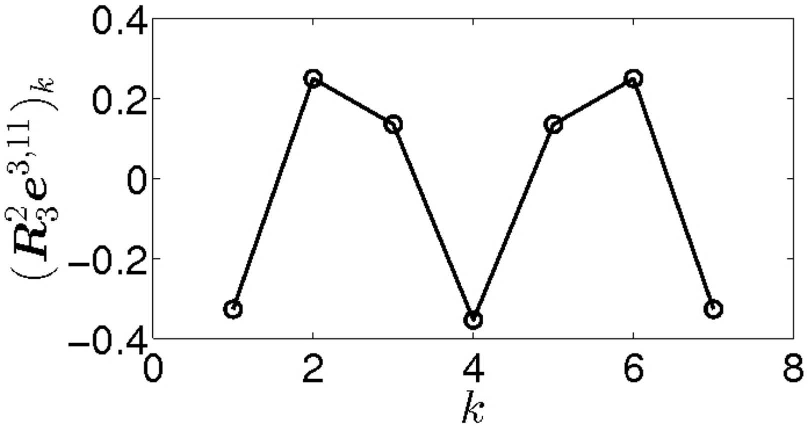

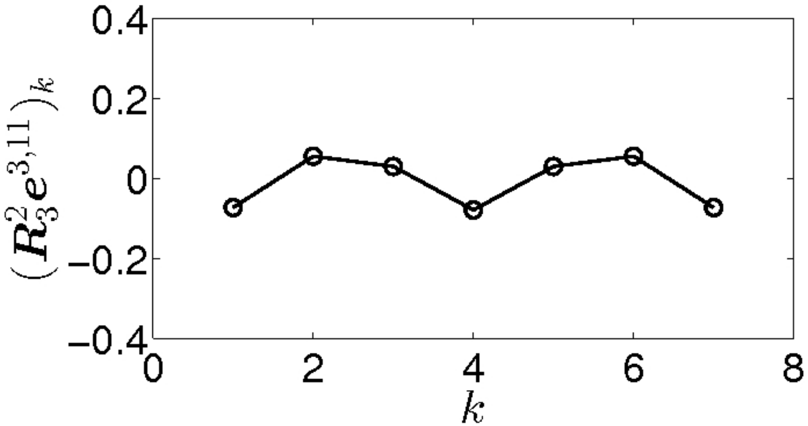

Analysis of the Linear Restriction

Theorem

The images of the Fourier modes $\boldsymbol{e}^{\ell,j}$, $j = 1, \ldots, N_\ell$ on Ω_ℓ concerning the **linear restriction** satisfy

$$\boldsymbol{R}_\ell^{\ell-1}\boldsymbol{e}^{\ell,j} = \frac{c_j}{\sqrt{2}}\boldsymbol{e}^{\ell-1,j} \quad \text{for } j \in \{1, \ldots, N_{\ell-1}\},$$

$$\boldsymbol{R}_\ell^{\ell-1}\boldsymbol{e}^{\ell,j} = \boldsymbol{0} \quad \text{for } j = N_{\ell-1} + 1,$$

$$\boldsymbol{R}_\ell^{\ell-1}\boldsymbol{e}^{\ell,j} = -\frac{s_{\bar{\jmath}}}{\sqrt{2}}\boldsymbol{e}^{\ell-1,\bar{\jmath}} \quad \text{for } j = N_\ell + 1 - \bar{\jmath} \text{ with } \bar{\jmath} \in \{1, \ldots, N_{\ell-1}\}.$$

with $c_j = \cos^2\left(j\pi\frac{h_\ell}{2}\right)$ and $s_{\bar{\jmath}} = \sin^2\left(\bar{\jmath}\pi\frac{h_\ell}{2}\right)$.

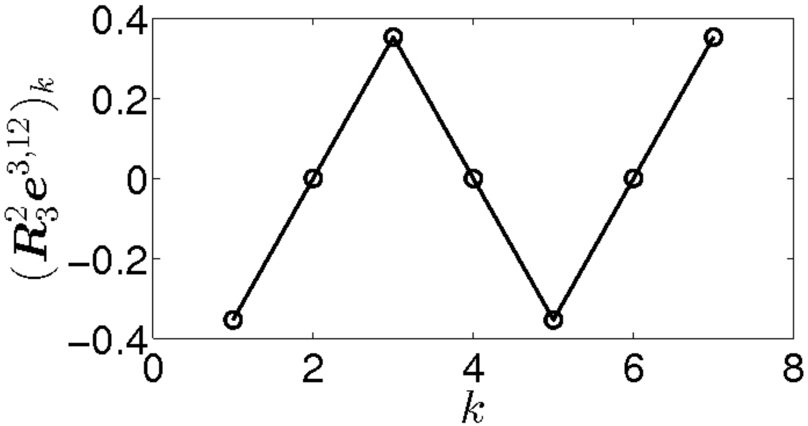

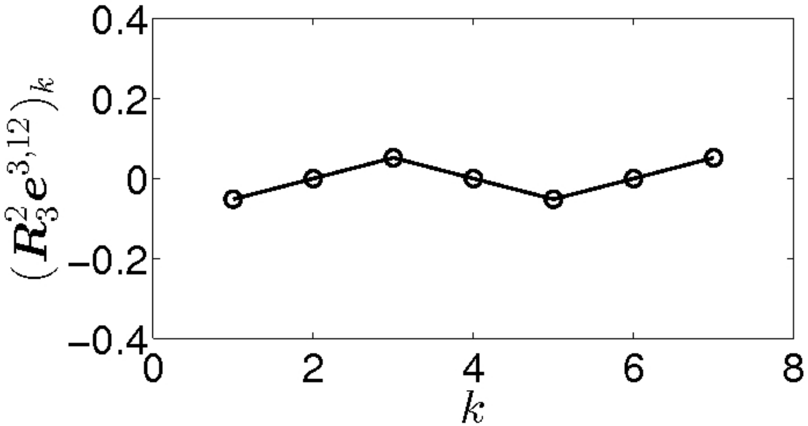

Analysis of the Linear Restriction

Theorem

The images of the Fourier modes $\boldsymbol{e}^{\ell,j}$, $j = 1, \ldots, N_\ell$ on Ω_ℓ concerning the **linear restriction** satisfy

$$\begin{aligned}
\boldsymbol{R}_\ell^{\ell-1}\boldsymbol{e}^{\ell,j} &= \frac{c_j}{\sqrt{2}}\boldsymbol{e}^{\ell-1,j} && \text{for } j \in \{1, \ldots, N_{\ell-1}\}, \\
\boldsymbol{R}_\ell^{\ell-1}\boldsymbol{e}^{\ell,j} &= \boldsymbol{0} && \text{for } j = N_{\ell-1} + 1, \\
\boldsymbol{R}_\ell^{\ell-1}\boldsymbol{e}^{\ell,j} &= -\frac{s_{\bar{\jmath}}}{\sqrt{2}}\boldsymbol{e}^{\ell-1,\bar{\jmath}} && \text{for } j = N_\ell + 1 - \bar{\jmath} \text{ with } \bar{\jmath} \in \{1, \ldots, N_{\ell-1}\}.
\end{aligned}$$

with $c_j = \cos^2\left(j\pi\frac{h_\ell}{2}\right)$ and $s_{\bar{\jmath}} = \sin^2\left(\bar{\jmath}\pi\frac{h_\ell}{2}\right)$.

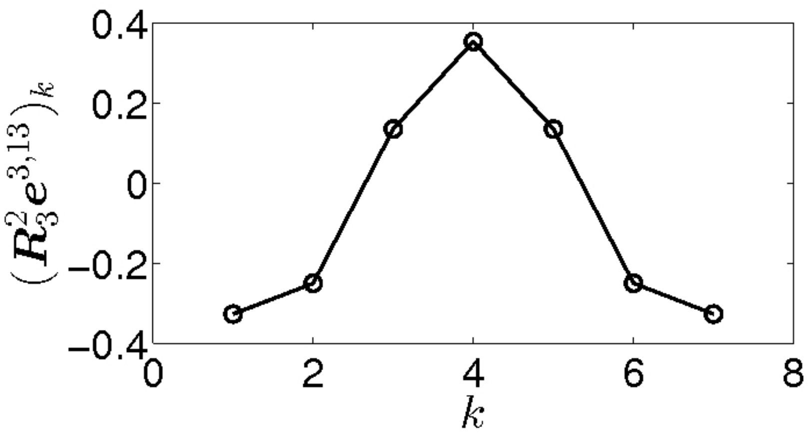

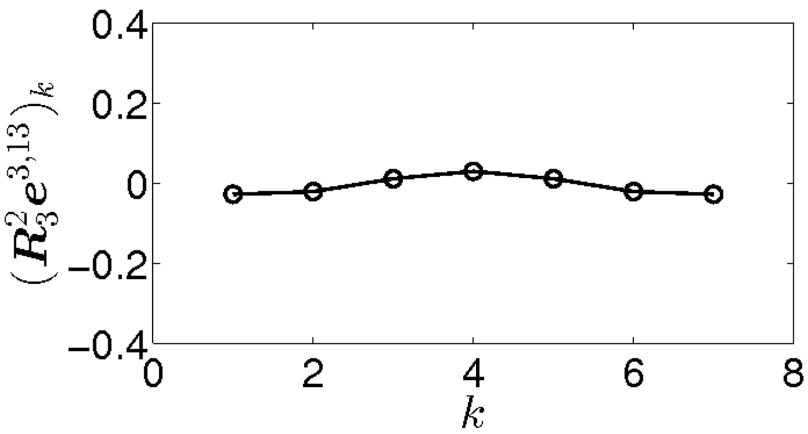

Analysis of the Linear Restriction

Theorem

The images of the Fourier modes $\boldsymbol{e}^{\ell,j}$, $j = 1, \ldots, N_\ell$ on Ω_ℓ concerning the **linear restriction** satisfy

$$\boldsymbol{R}_\ell^{\ell-1}\boldsymbol{e}^{\ell,j} = \frac{c_j}{\sqrt{2}}\boldsymbol{e}^{\ell-1,j} \quad \text{for } j \in \{1, \ldots, N_{\ell-1}\},$$

$$\boldsymbol{R}_\ell^{\ell-1}\boldsymbol{e}^{\ell,j} = \boldsymbol{0} \quad \text{for } j = N_{\ell-1} + 1,$$

$$\boldsymbol{R}_\ell^{\ell-1}\boldsymbol{e}^{\ell,j} = -\frac{s_{\bar{j}}}{\sqrt{2}}\boldsymbol{e}^{\ell-1,\bar{j}} \quad \text{for } j = N_\ell + 1 - \bar{j} \text{ with } \bar{j} \in \{1, \ldots, N_{\ell-1}\}.$$

with $c_j = \cos^2\left(j\pi\frac{h_\ell}{2}\right)$ and $s_{\bar{j}} = \sin^2\left(\bar{j}\pi\frac{h_\ell}{2}\right)$.

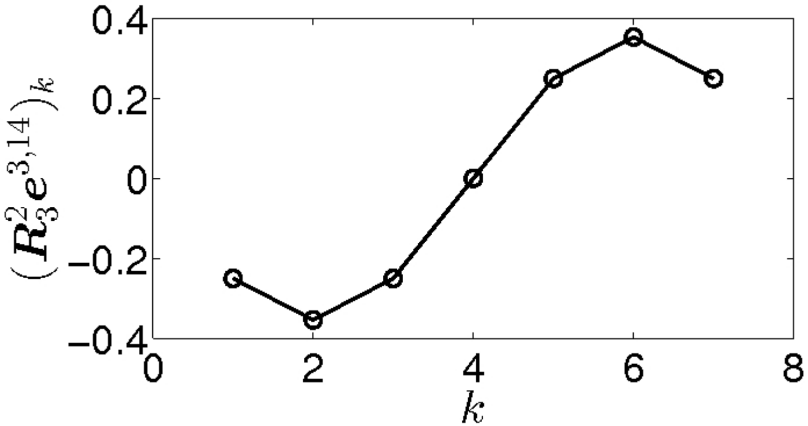

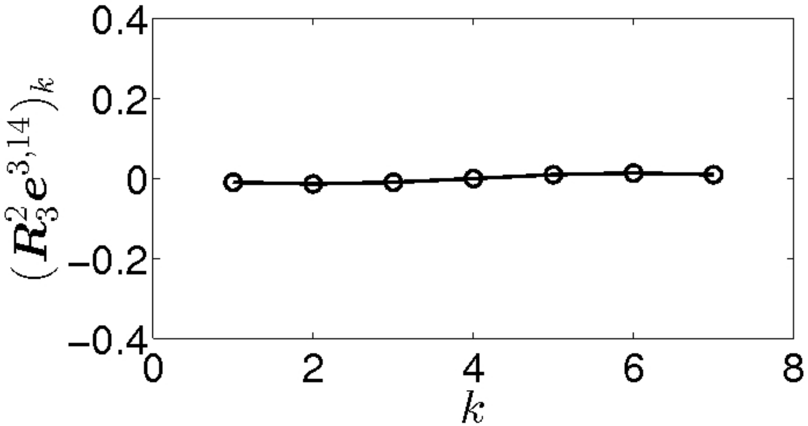

Analysis of the Linear Restriction

Theorem

The images of the Fourier modes $\boldsymbol{e}^{\ell,j}$, $j = 1, \dots, N_\ell$ on Ω_ℓ concerning the **linear restriction** satisfy

$$\begin{aligned}
\boldsymbol{R}_\ell^{\ell-1}\boldsymbol{e}^{\ell,j} &= \frac{c_j}{\sqrt{2}}\boldsymbol{e}^{\ell-1,j} && \text{for } j \in \{1,\dots,N_{\ell-1}\},\\
\boldsymbol{R}_\ell^{\ell-1}\boldsymbol{e}^{\ell,j} &= \boldsymbol{0} && \text{for } j = N_{\ell-1}+1,\\
\boldsymbol{R}_\ell^{\ell-1}\boldsymbol{e}^{\ell,j} &= -\frac{s_{\bar{\jmath}}}{\sqrt{2}}\boldsymbol{e}^{\ell-1,\bar{\jmath}} && \text{for } j = N_\ell + 1 - \bar{\jmath} \text{ with } \bar{\jmath} \in \{1,\dots,N_{\ell-1}\}.
\end{aligned}$$

with $c_j = \cos^2\left(j\pi\frac{h_\ell}{2}\right)$ and $s_{\bar{\jmath}} = \sin^2\left(\bar{\jmath}\pi\frac{h_\ell}{2}\right)$.

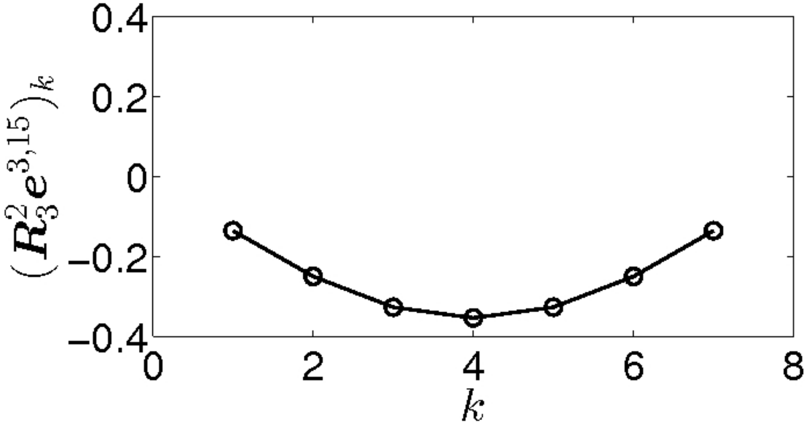

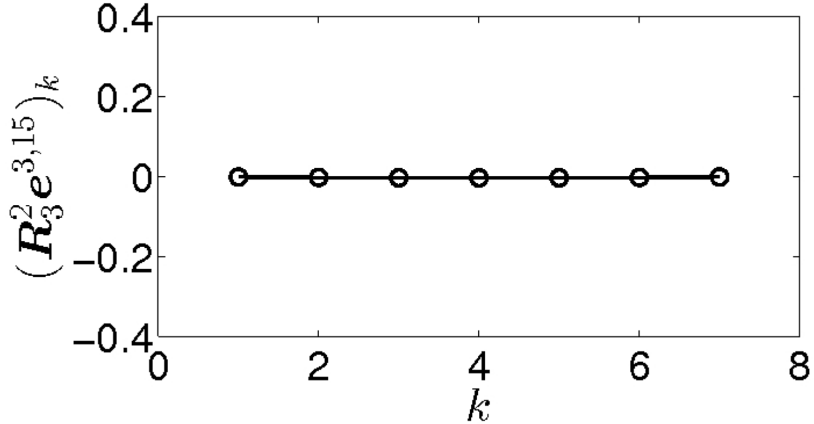

Mapping from $\Omega_{\ell-1}$ to Ω_ℓ (Prolongation)

Definition of the prolongation

A mapping

$$\boldsymbol{G} : \mathbb{R}^{N_{\ell-1}} \to \mathbb{R}^{N_\ell}$$

is called prolongation from $\Omega_{\ell-1}$ to Ω_ℓ, if it is linear und injective.

- Graphical presentation:

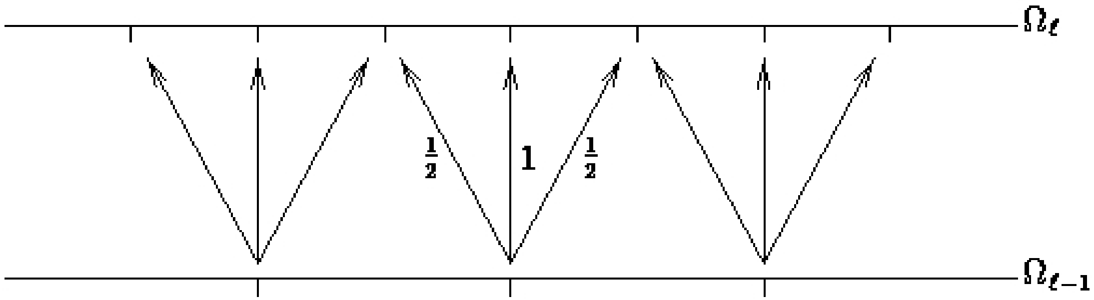

- Matrix representation:

$$\boldsymbol{P}_{\ell-1}^{\ell} = \frac{1}{2} \begin{pmatrix} 1 & & \\ 2 & & \\ 1 & 1 & \\ & 2 & \\ & 1 & \\ & & \ddots \end{pmatrix} \in \mathbb{R}^{N_\ell \times N_{\ell-1}}$$

Effect of the prolongation on the Fourier modes

Applying the prolongation to the scaled Fourier modes

$$\widetilde{\boldsymbol{e}}^{\ell,j} = \frac{1}{\sqrt{2h_\ell}} \boldsymbol{e}^{\ell,j}$$

yields

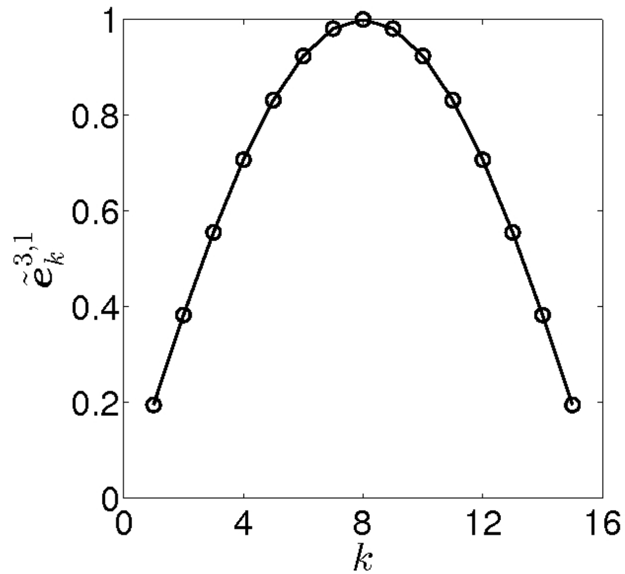

$\widetilde{\boldsymbol{e}}^{3,1}$

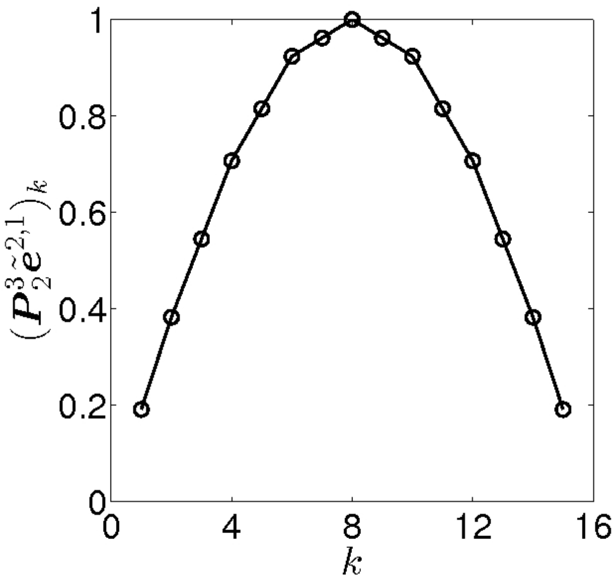

$\boldsymbol{P}_2^3 \widetilde{\boldsymbol{e}}^{2,1}$

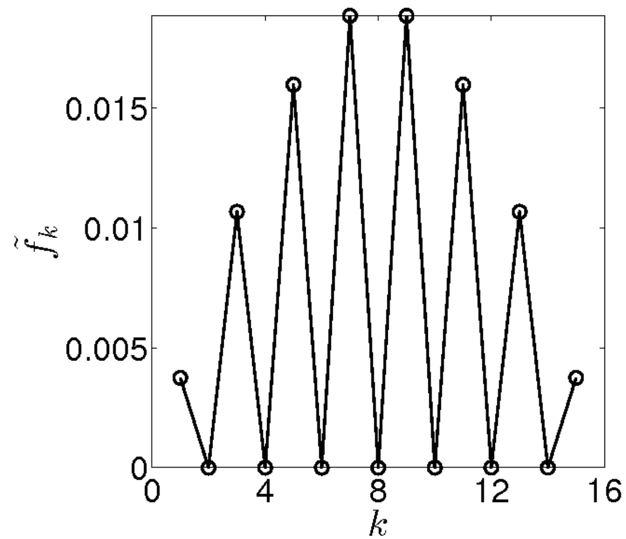

$\widetilde{\boldsymbol{e}}^{3,1} - \boldsymbol{P}_2^3 \widetilde{\boldsymbol{e}}^{2,1}$

Analysis of the linear prolongation

Theorem

The images of the Fourier modes $\boldsymbol{e}^{\ell-1,j}$, $j = 1, \ldots, N_{\ell-1}$ on $\Omega_{\ell-1}$ concerning the **linear prolongation** satisfy

$$\boldsymbol{P}_{\ell-1}^{\ell}\boldsymbol{e}^{\ell-1,j} = \sqrt{2}\left(c_j\boldsymbol{e}^{\ell,j} - s_j\boldsymbol{e}^{\ell,N_\ell+1-j}\right)$$

with $c_j = \cos^2\left(\frac{j\pi h_\ell}{2}\right)$ and $s_j = \sin^2\left(\frac{j\pi h_\ell}{2}\right)$.

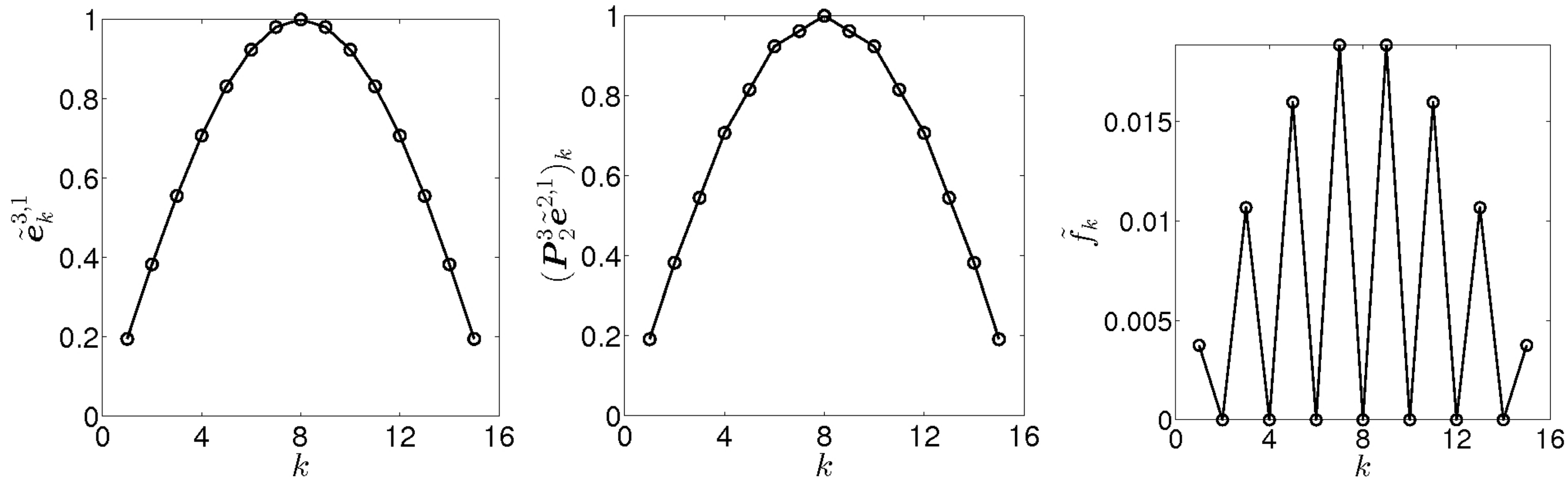

Two grid method

Let $\boldsymbol{e}_m^\ell = \boldsymbol{u}_m^\ell - \boldsymbol{u}^{\ell,*}$ (error), $\boldsymbol{d}_m^\ell = \boldsymbol{A}_\ell \boldsymbol{e}_m^\ell = \boldsymbol{A}_\ell \boldsymbol{u}_m^\ell - \boldsymbol{b}^\ell$ (defect)

1. Iterate $\boldsymbol{u}_m^\ell = \boldsymbol{M}_\ell \boldsymbol{u}_{m-1}^\ell + \boldsymbol{N}_\ell \boldsymbol{b}^\ell, \quad m = 1, ..., j$
2. Restrict the defect $\boldsymbol{d}^{\ell-1} = \boldsymbol{R}_\ell^{\ell-1} \boldsymbol{d}_m^\ell$
3. Solve $\boldsymbol{A}_{\ell-1} \boldsymbol{e}^{\ell-1} = \boldsymbol{d}^{\ell-1}$ exact
4. Prolongation of the result and correction of the approximate solution

Coarse grid correction

$$
\begin{aligned}
\boldsymbol{u}_m^{\ell,new} &= \boldsymbol{u}_m^\ell - \boldsymbol{P}_{\ell-1}^\ell \boldsymbol{e}^{\ell-1} \\
&= \boldsymbol{u}_m^\ell - \boldsymbol{P}_{\ell-1}^\ell \boldsymbol{A}_{\ell-1}^{-1} \boldsymbol{d}^{\ell-1} \\
&= \boldsymbol{u}_m^\ell - \boldsymbol{P}_{\ell-1}^\ell \boldsymbol{A}_{\ell-1}^{-1} \boldsymbol{R}_\ell^{\ell-1} \boldsymbol{d}_m^\ell \\
&= \boldsymbol{u}_m^\ell - \boldsymbol{P}_{\ell-1}^\ell \boldsymbol{A}_{\ell-1}^{-1} \boldsymbol{R}_\ell^{\ell-1} \left(\boldsymbol{A}_\ell \boldsymbol{u}_m^\ell - \boldsymbol{b}^\ell \right)
\end{aligned}
$$

Coarse grid correction effect on the error

Using

$$\boldsymbol{e}_m^\ell = \boldsymbol{u}_m^\ell - \boldsymbol{u}^{\ell,*} = \sum_{j=1}^{N_\ell} \alpha_j \boldsymbol{e}^{\ell,j} \text{ and } \Psi_\ell^{GGK}(\boldsymbol{e}) = (\boldsymbol{I} - \boldsymbol{P}_{\ell-1}^\ell \boldsymbol{A}_{\ell-1}^{-1} \boldsymbol{R}_\ell^{\ell-1} \boldsymbol{A}_\ell)\boldsymbol{e}$$

one obtains

$$\begin{aligned}
\boldsymbol{e}_m^{\ell,\text{new}} &= \boldsymbol{u}_m^{\ell,\text{new}} - \boldsymbol{u}^{\ell,*} \\
&= \boldsymbol{u}_m^\ell - \boldsymbol{u}^{\ell,*} - \boldsymbol{P}_{\ell-1}^\ell \boldsymbol{A}_{\ell-1}^{-1} \boldsymbol{R}_\ell^{\ell-1} \left(\boldsymbol{A}_\ell \boldsymbol{u}_m^\ell - \boldsymbol{b}^\ell \right) \\
&= \boldsymbol{e}_m^\ell - \boldsymbol{P}_{\ell-1}^\ell \boldsymbol{A}_{\ell-1}^{-1} \boldsymbol{R}_\ell^{\ell-1} \boldsymbol{A}_\ell \boldsymbol{e}_m^\ell \\
&= \Psi_\ell^{GGK} \left(\boldsymbol{e}_m^\ell \right) \\
&= \sum_{j=1}^{N_\ell} \alpha_j \Psi_\ell^{GGK} \left(\boldsymbol{e}^{\ell,j} \right)
\end{aligned}$$

Coarse grid correction effect on the Fourier modes

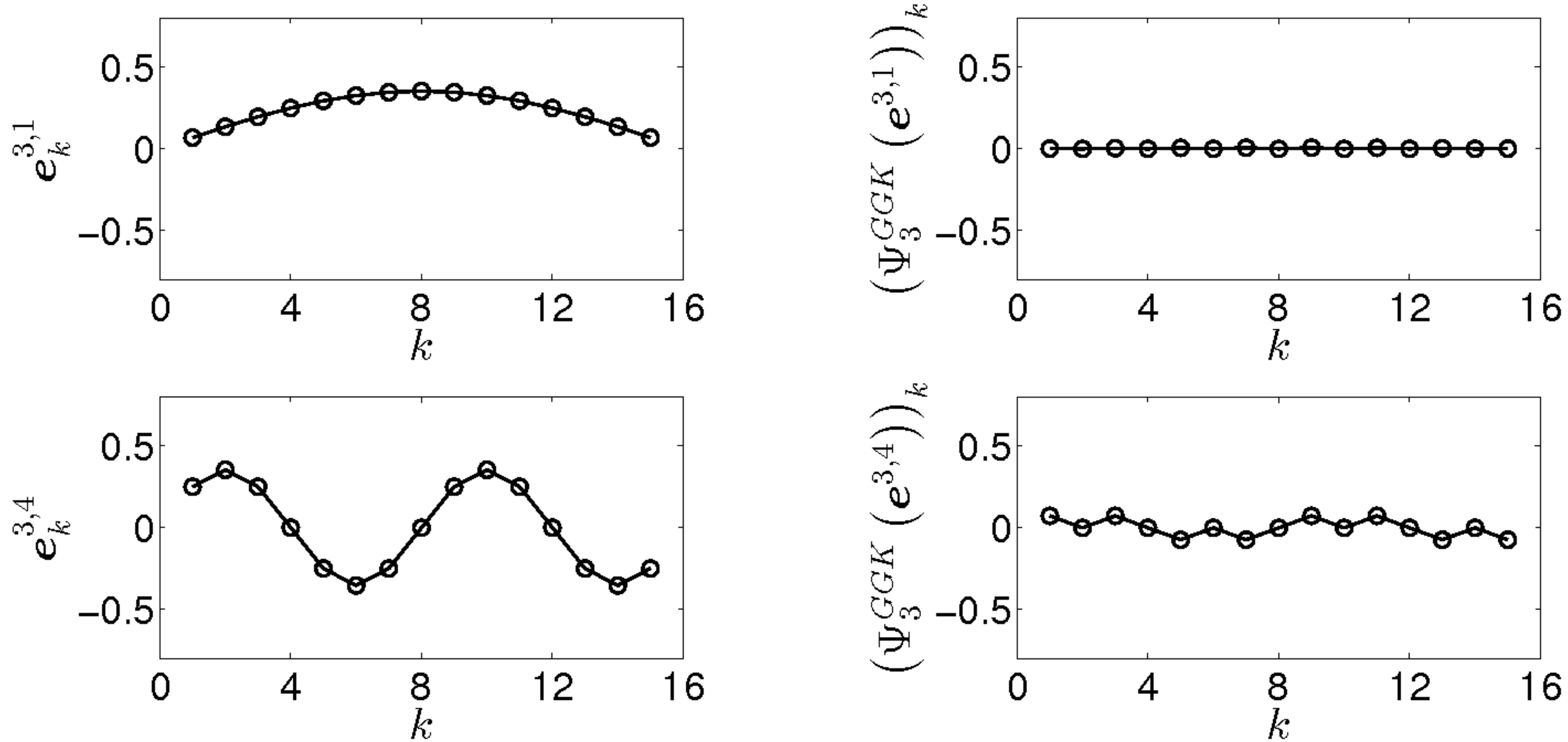

Fourier mode

Image under coarse grid correction

Coarse grid correction effect on the Fourier modes

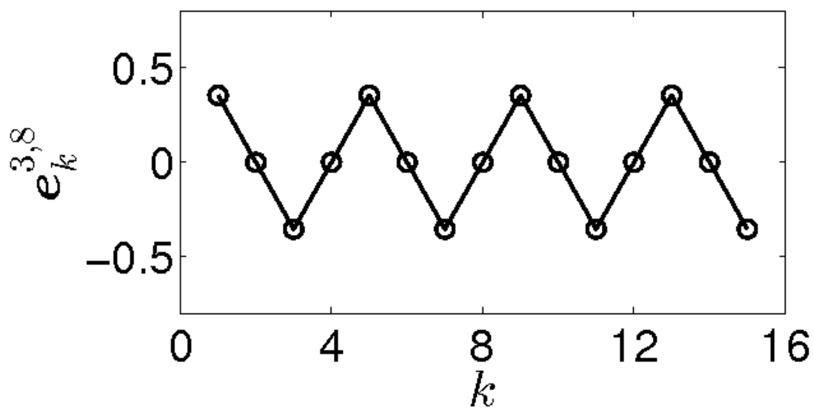

Fourier mode

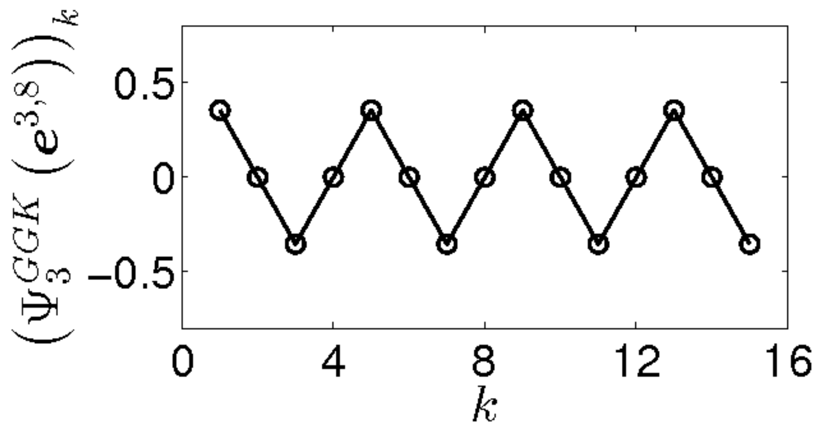

Image under coarse grid correction

Coarse grid correction effect on the Fourier modes

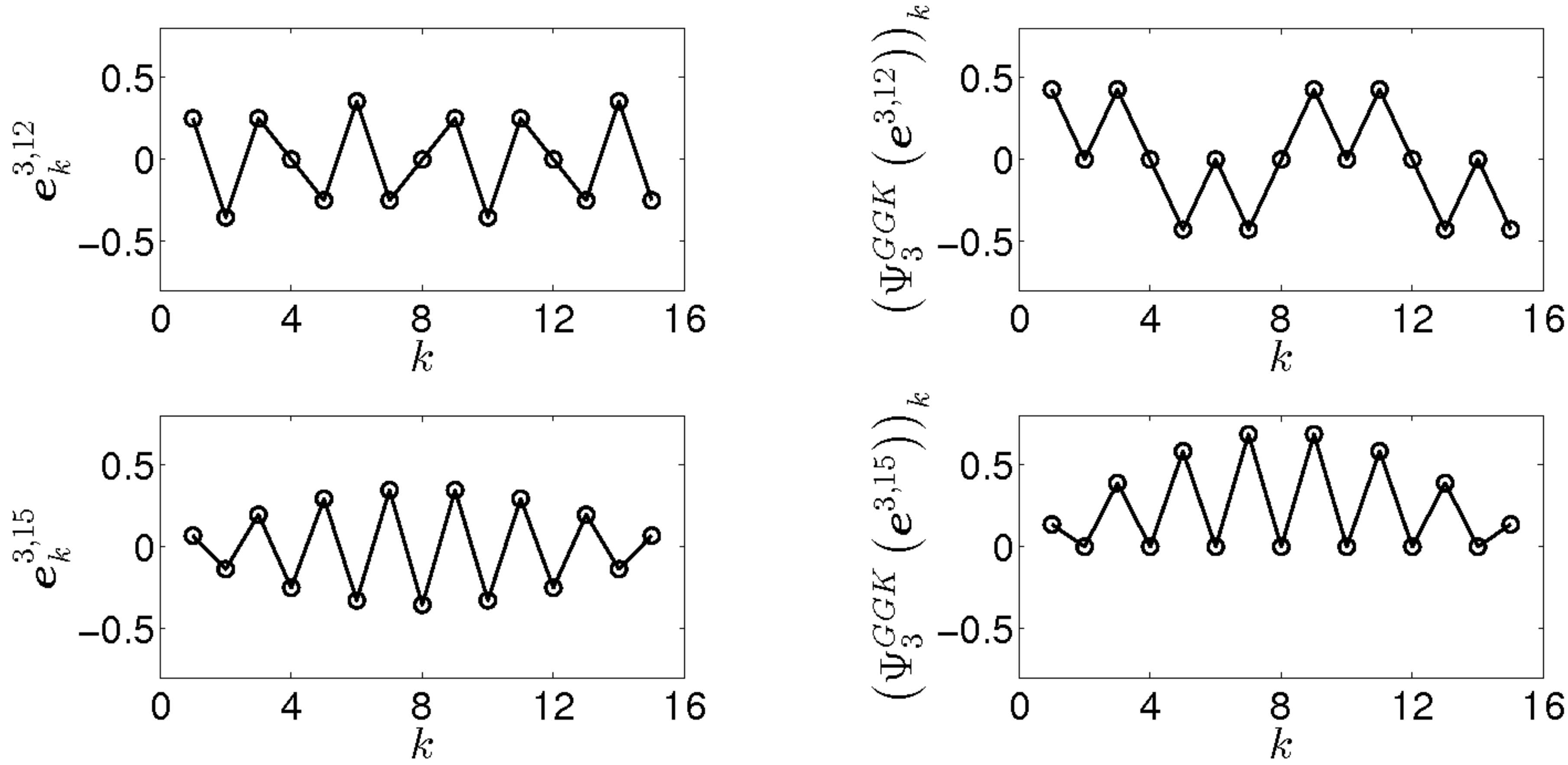

Fourier mode

Image under coarse grid correction

Analysis of the coarse grid correction

Theorem

The images of the Fourier modes $\boldsymbol{e}^{\ell,j}$, $j = 1, \dots, N_\ell$ on Ω_ℓ w.r.t. the **coarse grid correction** with linear restriction and prolongation satisfy

$$
\begin{aligned}
\Psi_\ell^{GGK}\left(\boldsymbol{e}^{\ell,j}\right) &= \quad s_j\, \boldsymbol{e}^{\ell,j} + s_j\, \boldsymbol{e}^{\ell,\bar{\jmath}} && \text{for } j \in \{1, \dots, N_{\ell-1}\} \text{ and } \bar{\jmath} = N_\ell + 1 - j, \\
\Psi_\ell^{GGK}\left(\boldsymbol{e}^{\ell,j}\right) &= \quad \boldsymbol{e}^{\ell,j} && \text{for } j = N_{\ell-1} + 1, \\
\Psi_\ell^{GGK}\left(\boldsymbol{e}^{\ell,j}\right) &= \quad c_{\bar{\jmath}}\, \boldsymbol{e}^{\ell,j} + c_{\bar{\jmath}}\, \boldsymbol{e}^{\ell,\bar{\jmath}} && \text{for } j = N_\ell + 1 - \bar{\jmath} \text{ with } \bar{\jmath} \in \{1, \dots, N_{\ell-1}\}
\end{aligned}
$$

where $c_{\bar{\jmath}} = \cos^2(\bar{\jmath}\pi h_\ell/2)$ and $s_j = \sin^2(j\pi h_\ell/2)$.

Analysis of the coarse grid correction

Theorem

The images of the Fourier modes $\mathbf{e}^{\ell,j}$, $j = 1, \ldots, N_\ell$ on Ω_ℓ w.r.t. the **coarse grid correction** with linear restriction and prolongation satisfy

$$\Psi_\ell^{GGK}\left(\mathbf{e}^{\ell,j}\right) = s_j\, \mathbf{e}^{\ell,j} + s_j\, \mathbf{e}^{\ell,\bar{\jmath}} \quad \text{for } j \in \{1, \ldots, N_{\ell-1}\} \text{ and } \bar{\jmath} = N_\ell + 1 - j,$$

$$\Psi_\ell^{GGK}\left(\mathbf{e}^{\ell,j}\right) = \mathbf{e}^{\ell,j} \quad \text{for } j = N_{\ell-1} + 1,$$

$$\Psi_\ell^{GGK}\left(\mathbf{e}^{\ell,j}\right) = c_{\bar{\jmath}}\, \mathbf{e}^{\ell,j} + c_{\bar{\jmath}}\, \mathbf{e}^{\ell,\bar{\jmath}} \quad \text{for } j = N_\ell + 1 - \bar{\jmath} \text{ with } \bar{\jmath} \in \{1, \ldots, N_{\ell-1}\}$$

where $c_{\bar{\jmath}} = \cos^2(\bar{\jmath}\pi h_\ell/2)$ and $s_j = \sin^2(j\pi h_\ell/2)$.

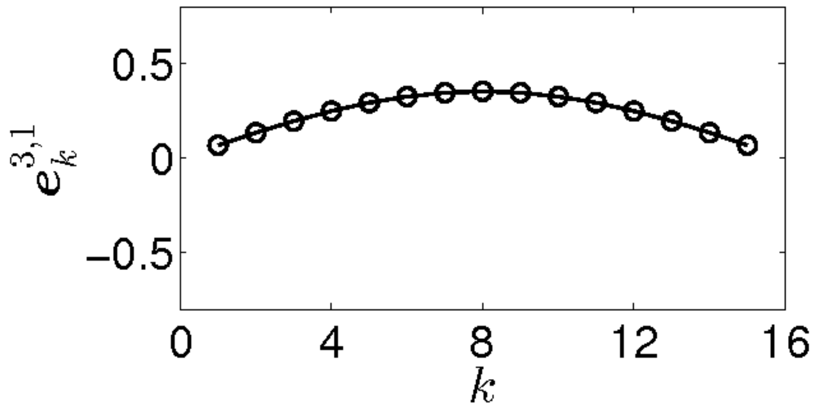

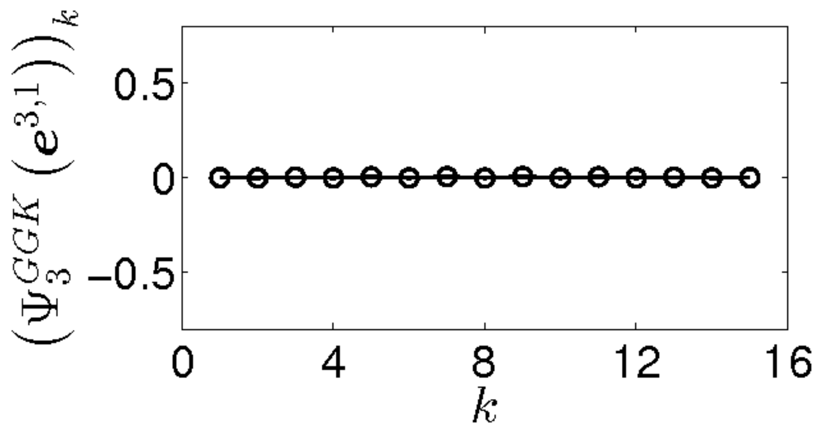

Analysis of the coarse grid correction

Theorem

The images of the Fourier modes $\mathbf{e}^{\ell,j}$, $j = 1, \ldots, N_\ell$ on Ω_ℓ w.r.t. the **coarse grid correction** with linear restriction and prolongation satisfy

$$\begin{aligned}
\Psi_\ell^{GGK}\left(\mathbf{e}^{\ell,j}\right) &= s_j\, \mathbf{e}^{\ell,j} + s_j\, \mathbf{e}^{\ell,\bar{\jmath}} && \text{for } j \in \{1, \ldots, N_{\ell-1}\} \text{ and } \bar{\jmath} = N_\ell + 1 - j, \\
\Psi_\ell^{GGK}\left(\mathbf{e}^{\ell,j}\right) &= \mathbf{e}^{\ell,j} && \text{for } j = N_{\ell-1} + 1, \\
\Psi_\ell^{GGK}\left(\mathbf{e}^{\ell,j}\right) &= c_{\bar{\jmath}}\, \mathbf{e}^{\ell,j} + c_{\bar{\jmath}}\, \mathbf{e}^{\ell,\bar{\jmath}} && \text{for } j = N_\ell + 1 - \bar{\jmath} \text{ with } \bar{\jmath} \in \{1, \ldots, N_{\ell-1}\}
\end{aligned}$$

where $c_{\bar{\jmath}} = \cos^2(\bar{\jmath}\pi h_\ell/2)$ and $s_j = \sin^2(j\pi h_\ell/2)$.

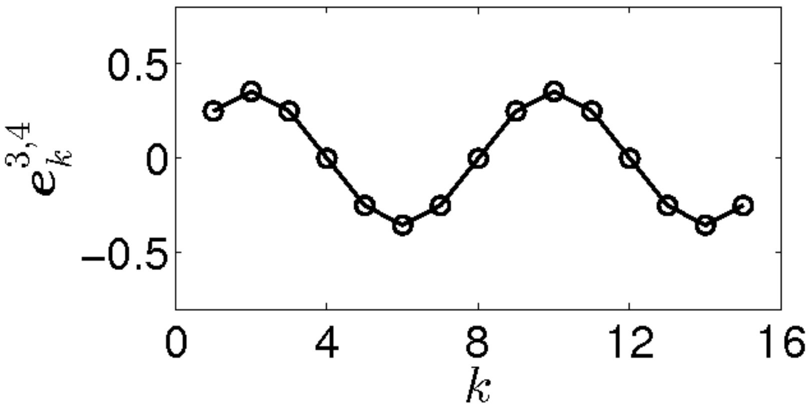

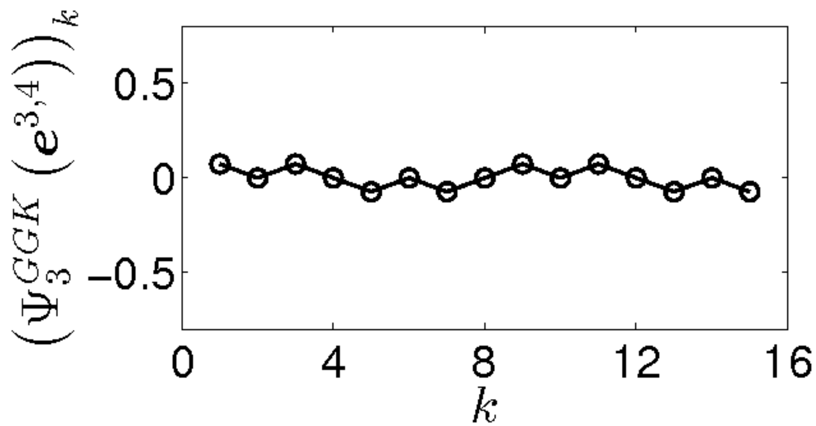

Analysis of the coarse grid correction

Theorem

The images of the Fourier modes $\boldsymbol{e}^{\ell,j}$, $j = 1, \ldots, N_\ell$ on Ω_ℓ w.r.t. the **coarse grid correction** with linear restriction and prolongation satisfy

$$\begin{aligned}
\Psi_\ell^{GGK}\left(\boldsymbol{e}^{\ell,j}\right) &= s_j\, \boldsymbol{e}^{\ell,j} + s_j\, \boldsymbol{e}^{\ell,\bar{\jmath}} && \text{for } j \in \{1, \ldots, N_{\ell-1}\} \text{ and } \bar{\jmath} = N_\ell + 1 - j,\\
\Psi_\ell^{GGK}\left(\boldsymbol{e}^{\ell,j}\right) &= \boldsymbol{e}^{\ell,j} && \text{for } j = N_{\ell-1} + 1,\\
\Psi_\ell^{GGK}\left(\boldsymbol{e}^{\ell,j}\right) &= c_{\bar{\jmath}}\, \boldsymbol{e}^{\ell,j} + c_{\bar{\jmath}}\, \boldsymbol{e}^{\ell,\bar{\jmath}} && \text{for } j = N_\ell + 1 - \bar{\jmath} \text{ with } \bar{\jmath} \in \{1, \ldots, N_{\ell-1}\}
\end{aligned}$$

where $c_{\bar{\jmath}} = \cos^2(\bar{\jmath}\pi h_\ell/2)$ and $s_j = \sin^2(j\pi h_\ell/2)$.

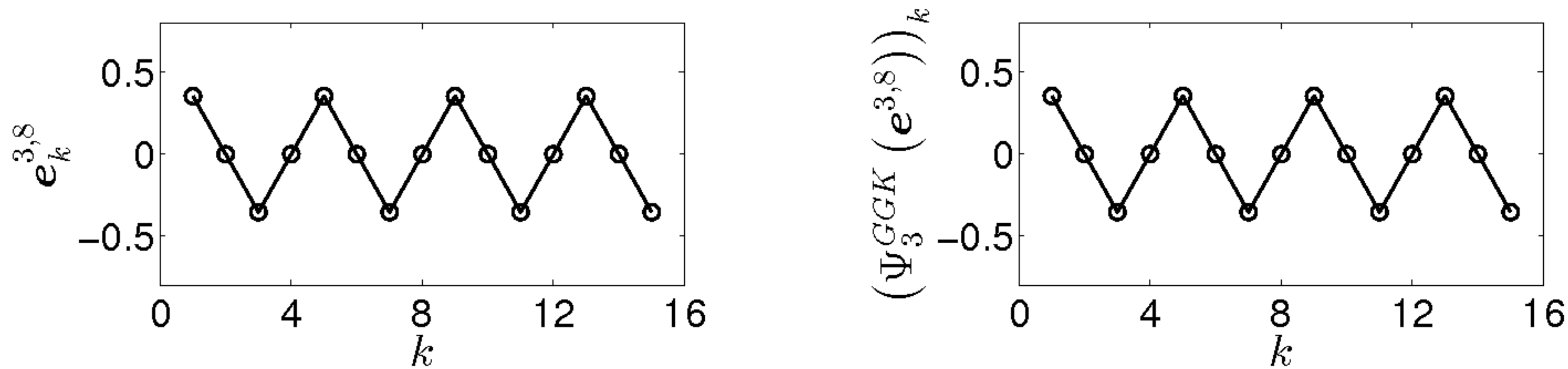

Analysis of the coarse grid correction

Theorem

The images of the Fourier modes $\boldsymbol{e}^{\ell,j}$, $j = 1, \ldots, N_\ell$ on Ω_ℓ w.r.t. the **coarse grid correction** with linear restriction and prolongation satisfy

$$\Psi_\ell^{GGK}\left(\boldsymbol{e}^{\ell,j}\right) = s_j\, \boldsymbol{e}^{\ell,j} + s_j\, \boldsymbol{e}^{\ell,\bar{\jmath}} \text{ for } j \in \{1, \ldots, N_{\ell-1}\} \text{ and } \bar{\jmath} = N_\ell + 1 - j,$$

$$\Psi_\ell^{GGK}\left(\boldsymbol{e}^{\ell,j}\right) = \boldsymbol{e}^{\ell,j} \text{ for } j = N_{\ell-1} + 1,$$

$$\Psi_\ell^{GGK}\left(\boldsymbol{e}^{\ell,j}\right) = c_{\bar{\jmath}}\, \boldsymbol{e}^{\ell,j} + c_{\bar{\jmath}}\, \boldsymbol{e}^{\ell,\bar{\jmath}} \text{ for } j = N_\ell + 1 - \bar{\jmath} \text{ with } \bar{\jmath} \in \{1, \ldots, N_{\ell-1}\}$$

where $c_{\bar{\jmath}} = \cos^2(\bar{\jmath}\pi h_\ell/2)$ and $s_j = \sin^2(j\pi h_\ell/2)$.

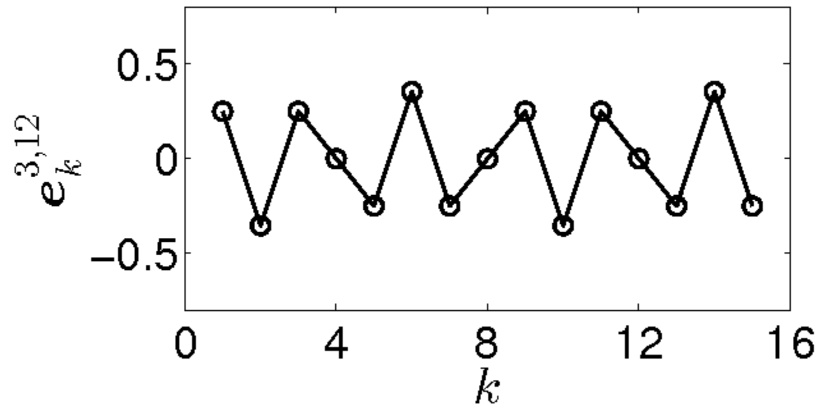

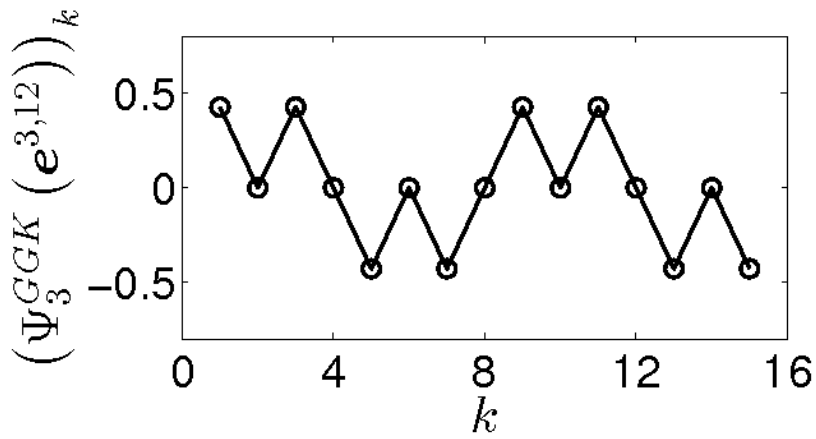

Analysis of the coarse grid correction

Theorem

The images of the Fourier modes $\mathbf{e}^{\ell,j}$, $j = 1, \ldots, N_\ell$ on Ω_ℓ w.r.t. the **coarse grid correction** with linear restriction and prolongation satisfy

$$\begin{aligned}
\Psi_\ell^{GGK}\left(\mathbf{e}^{\ell,j}\right) &= s_j\,\mathbf{e}^{\ell,j} + s_j\,\mathbf{e}^{\ell,\bar{\jmath}} && \text{for } j \in \{1,\ldots,N_{\ell-1}\} \text{ and } \bar{\jmath} = N_\ell + 1 - j,\\
\Psi_\ell^{GGK}\left(\mathbf{e}^{\ell,j}\right) &= \mathbf{e}^{\ell,j} && \text{for } j = N_{\ell-1} + 1,\\
\Psi_\ell^{GGK}\left(\mathbf{e}^{\ell,j}\right) &= c_{\bar{\jmath}}\,\mathbf{e}^{\ell,j} + c_{\bar{\jmath}}\,\mathbf{e}^{\ell,\bar{\jmath}} && \text{for } j = N_\ell + 1 - \bar{\jmath} \text{ with } \bar{\jmath} \in \{1,\ldots,N_{\ell-1}\}
\end{aligned}$$

where $c_{\bar{\jmath}} = \cos^2(\bar{\jmath}\pi h_\ell/2)$ and $s_j = \sin^2(j\pi h_\ell/2)$.

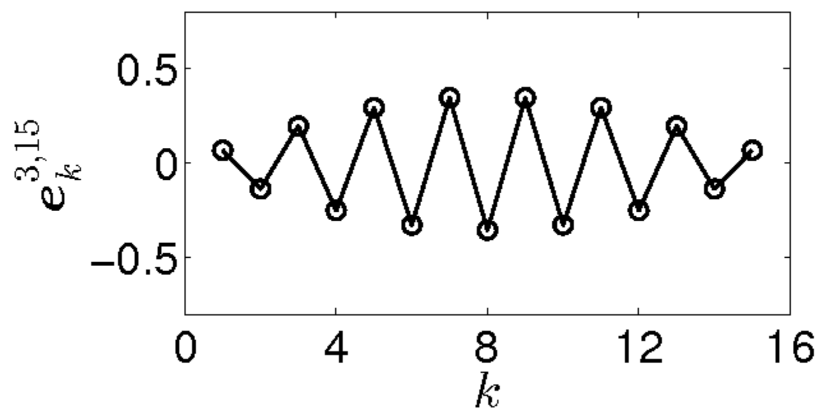

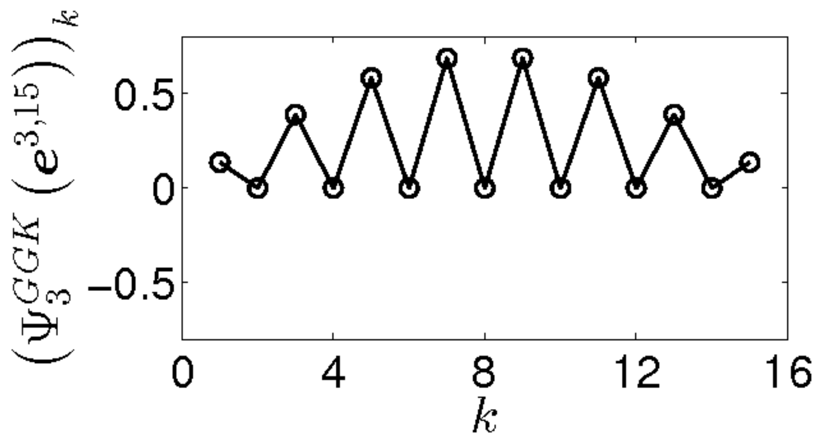

Two grid method

For $i = 1, \ldots, \nu_1$
$u^\ell := \phi_\ell \left(u^\ell, f^\ell \right)$
$d^{\ell-1} := R_\ell^{\ell-1} \left(A_\ell u^\ell - f^\ell \right)$
$e^{\ell-1} := A_{\ell-1}^{-1} d^{\ell-1}$
$u^\ell := u^\ell - P_{\ell-1}^\ell e^{\ell-1}$
For $i = 1, \ldots, \nu_2$
$u^\ell := \phi_\ell \left(u^\ell, f^\ell \right)$

Two grid method

- ν_1 number of steps for pre-smoothing
- ν_2 number of steps for post-smoothing
- Graphical presentation

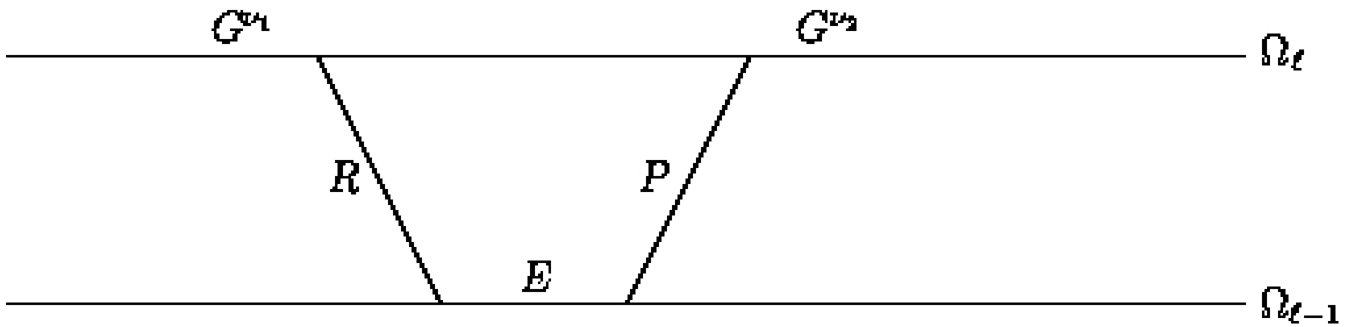

Two grid method - damped Jacobi method ($\omega = 1/4$)

Development of the error

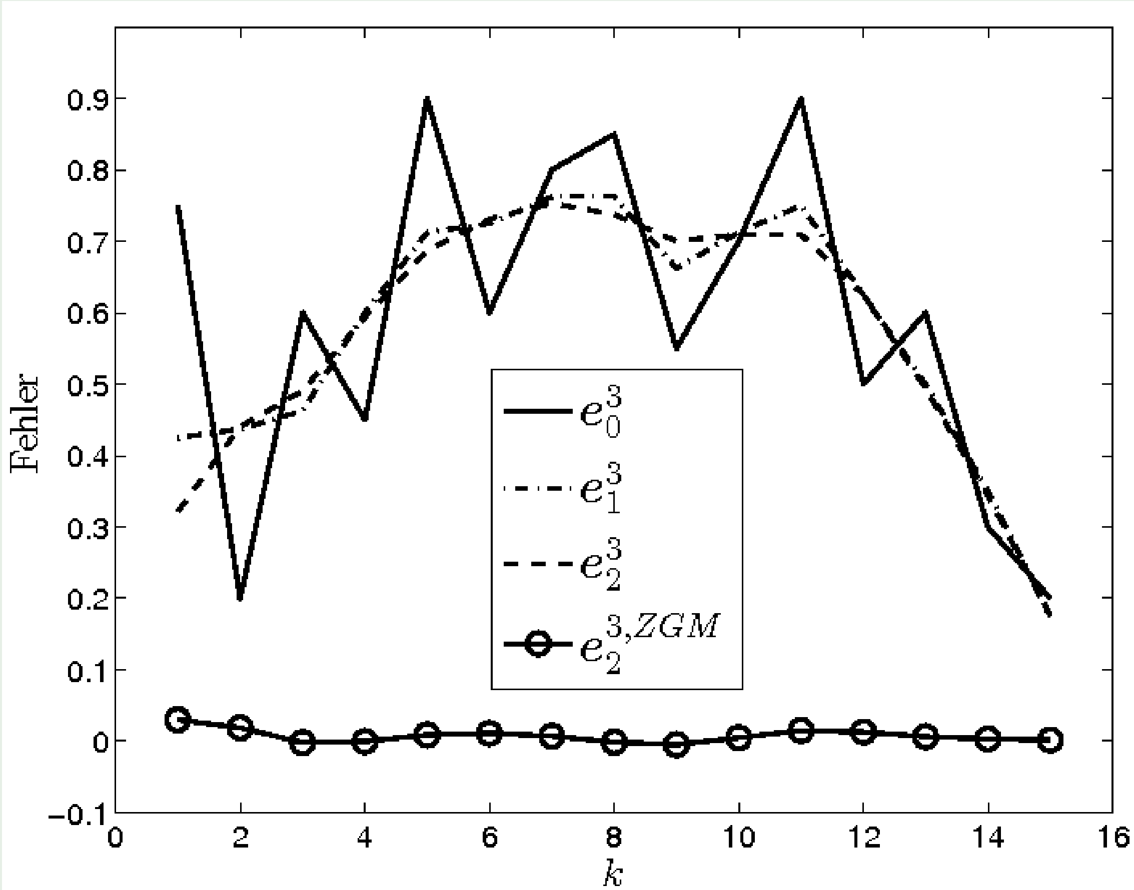

$$\boldsymbol{e}_0^3 := (0.75,\ 0.2,\ 0.6,\ 0.45,\ 0.9,\ 0.6,\ 0.8,\ 0.85,\ 0.55,\ 0.7,\ 0.9,\ 0.5,\ 0.6,\ 0.3,\ 0.2)^T \in \mathbb{R}^{15}$$

Analysis of the two grid method

Theorem

Let the two grid method be defined by damped Jacobi method in combination with linear restriction and linear prolongation. Then the images of the Fourier modes $\boldsymbol{e}^{\ell,j}$, $j = 1,\dots,N_\ell$ on Ω_ℓ satisfy

$$\Psi_\ell^{ZGM(\nu_1,\nu_2)}\left(\boldsymbol{e}^{\ell,j}\right) = (\lambda^{\ell,j})^{\nu_1} s_j \left((\lambda^{\ell,j})^{\nu_2}\boldsymbol{e}^{\ell,j} + (\lambda^{\ell,\bar{\jmath}})^{\nu_2}\boldsymbol{e}^{\ell,\bar{\jmath}}\right)$$
$$\text{for } j \in \{1,\dots,N_{\ell-1}\} \text{ and } \bar{\jmath} = N_\ell + 1 - j,$$
$$\Psi_\ell^{ZGM(\nu_1,\nu_2)}\left(\boldsymbol{e}^{\ell,j}\right) = (\lambda^{\ell,j})^{\nu_1+\nu_2}\boldsymbol{e}^{\ell,j} \quad \text{for } j = N_{\ell-1}+1,$$
$$\Psi_\ell^{ZGM(\nu_1,\nu_2)}\left(\boldsymbol{e}^{\ell,j}\right) = (\lambda^{\ell,j})^{\nu_1} c_{\bar{\jmath}} \left((\lambda^{\ell,j})^{\nu_2}\boldsymbol{e}^{\ell,j} + (\lambda^{\ell,\bar{\jmath}})^{\nu_2}\boldsymbol{e}^{\ell,\bar{\jmath}}\right)$$
$$\text{for } j = N_\ell + 1 - \bar{\jmath} \text{ with } \bar{\jmath} \in \{1,\dots,N_{\ell-1}\},$$

where $c_{\bar{\jmath}} = \cos^2\left(\bar{\jmath}\pi\frac{h_\ell}{2}\right)$, $s_j = \sin^2\left(j\pi\frac{h_\ell}{2}\right)$, $\lambda^{\ell,j} = \lambda^{\ell,j}(1/4)$ and $\lambda^{\ell,\bar{\jmath}} = \lambda^{\ell,\bar{\jmath}}(1/4)$.

Multigrid method

- Problem: Two grid method is usually not workable
- Extension:
  - Solve $\boldsymbol{A}_{\ell-1}\boldsymbol{e}^{\ell-1} = \boldsymbol{d}^{\ell-1}$ approximately on $\Omega_{\ell-1}$ (sufficient, since $\boldsymbol{P}_{\ell-1}^{\ell}\boldsymbol{A}_{\ell-1}^{-1}\boldsymbol{d}^{\ell-1} \approx \boldsymbol{e}^{\ell}$)
  - Employ a two grid method on $\Omega_{\ell-1}$

    $\Rightarrow$ three grid method
  - Carry forward to obtain a $\ell + 1$ grid method and solve

$$\boldsymbol{A}_0\boldsymbol{e}^0 = \boldsymbol{d}^0$$

exact.

Multigrid method

$\ell = 0$

Y:

- $u^0 := A_0^{-1} f^0$
- Output u^0

N:

- For $i = 1, \ldots, \nu_1$
  - $u^\ell := \phi_\ell \left(u^\ell, f^\ell \right)$
- $d^{\ell-1} := R_\ell^{\ell-1} \left(A_\ell u^\ell - f^\ell \right)$
- $e_0^{\ell-1} := \mathbf{0}$
- For $i = 1, \ldots, \gamma$
  - $e_i^{\ell-1} := \phi_{\ell-1}^{\mathrm{MGM}(\nu_1,\nu_2)} \left(e_{i-1}^{\ell-1}, d^{\ell-1} \right)$
- $u^\ell := u^\ell - P_{\ell-1}^\ell e_\gamma^{\ell-1}$
- For $i = 1, \ldots, \nu_2$
  - $u^\ell := \phi_\ell \left(u^\ell, f^\ell \right)$
- Output u^ℓ

Multigrid method

- V-cycle $\gamma = 1,\ l = 3$:

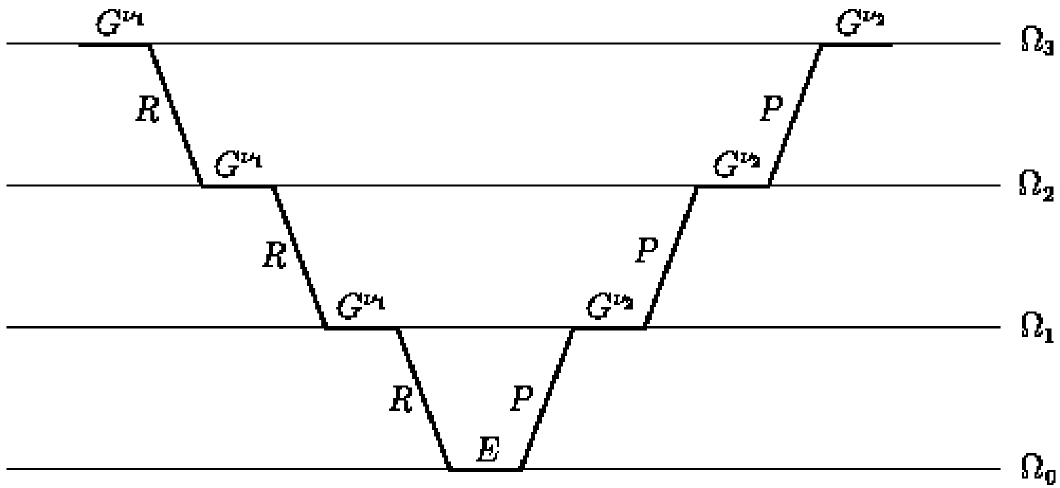

- W-cycle $\gamma = 2,\ l = 3$:

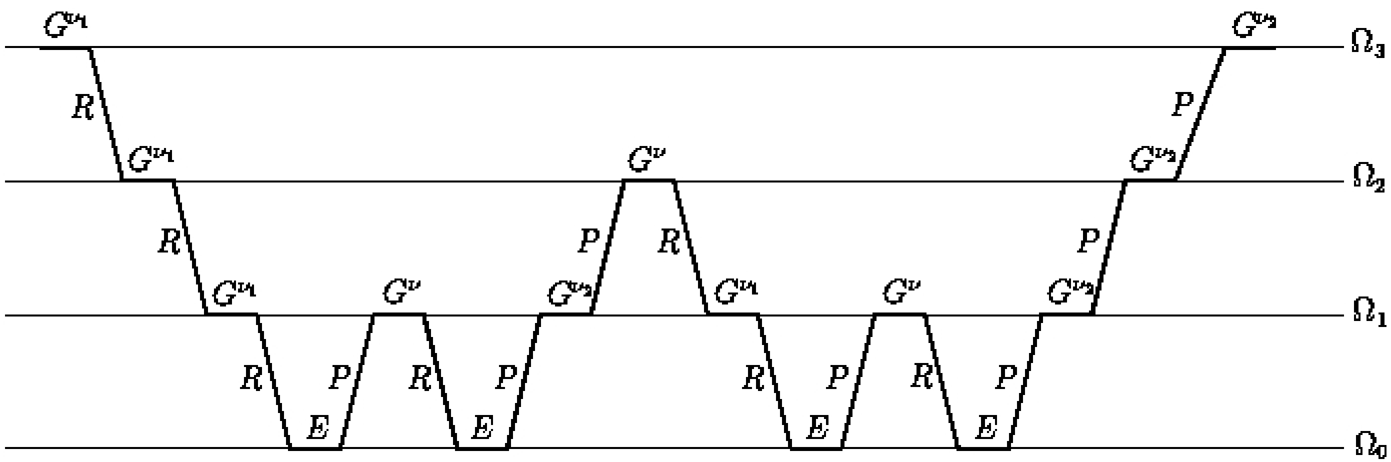

Multigrid method - damped Jacobi method ($\omega = 1/4$)

Poisson's equation

$$\begin{aligned} -u''(x) &= f(x) \quad \text{for } x \in \Omega, \\ u(x) &= 0 \quad \text{for } x \in \partial\Omega = \{0, 1\} \end{aligned}$$

where

$$f(x) = \frac{\pi^2}{8}\left(9\sin\left(\frac{3\pi x}{2}\right) + 25\sin\left(\frac{5\pi x}{2}\right)\right)$$

Exact solution

$$u(x) = \sin(2\pi x)\cos\left(\frac{\pi x}{2}\right)$$

Initialization

$$\boldsymbol{u}_0^3 = (u(x_1), \cdots, u(x_{N_3}))^T - \boldsymbol{e}_0^3 \quad \text{with} \quad x_i = ih_3$$

using

$$\boldsymbol{e}_0^3 := (0.75,\ 0.2,\ 0.6,\ 0.45,\ 0.9,\ 0.6,\ 0.8,\ 0.85,\ 0.55,\ 0.7,\ 0.9,\ 0.5,\ 0.6,\ 0.3,\ 0.2)^T \in \mathbb{R}^{15}$$

Multigrid method - damped Jacobi method ($\omega = 1/4$)

Poisson's equation - V-cycle

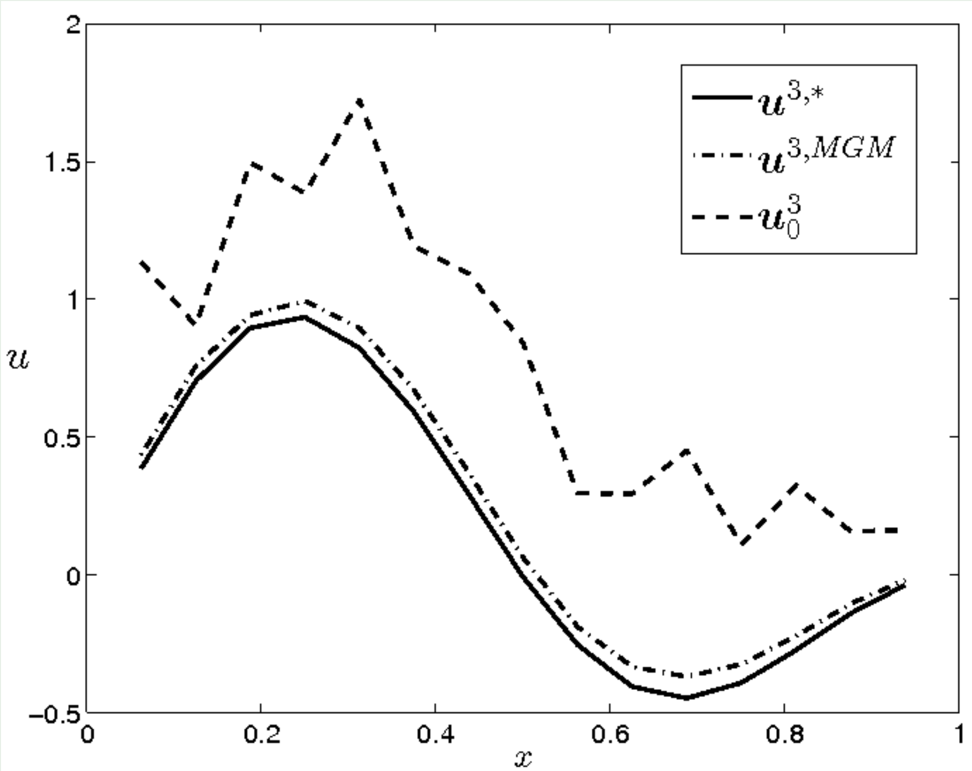

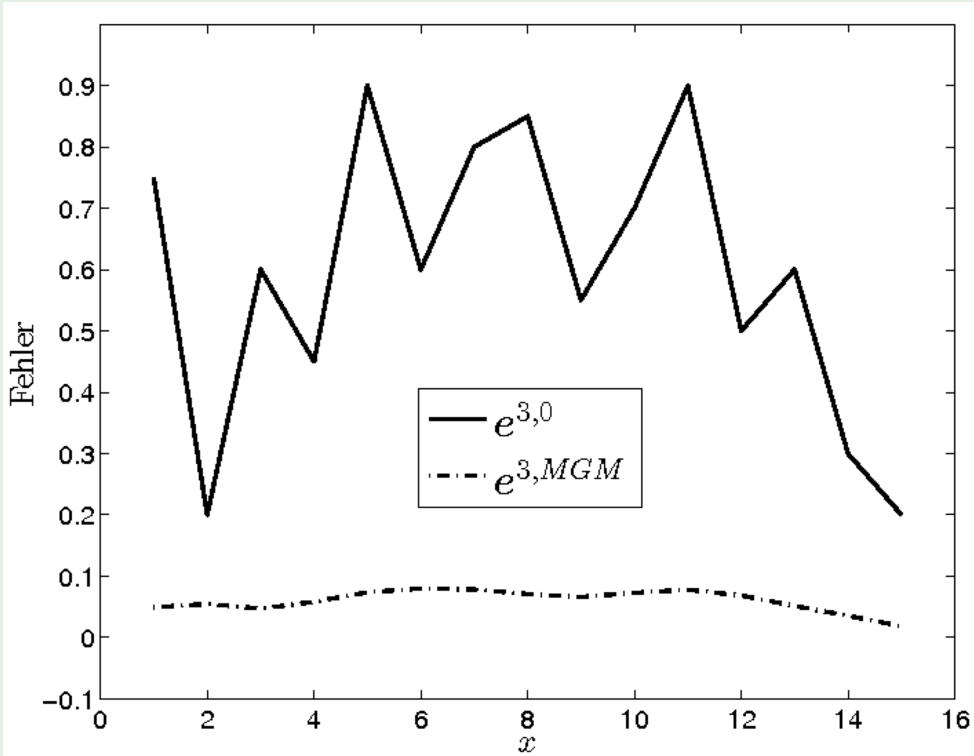

Multigrid method - damped Jacobi method ($\omega = 1/4$)

Poisson's equation - W-cycle

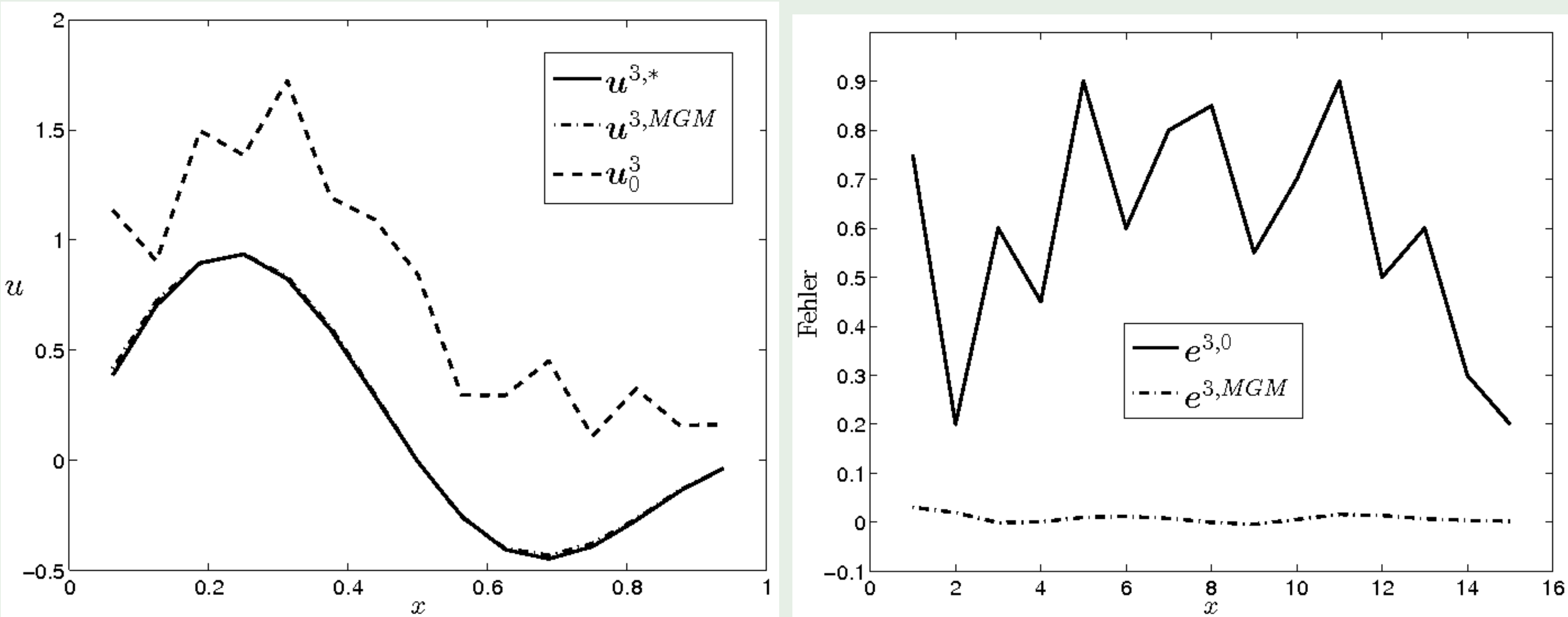

Multigrid method versus Jacobi method

Poisson's equation - Percentage comparison - Run times

Computational effort			
Mesh	Number of Unknowns	Multigrid method	Classical Jacobi method
Ω_2	7	100 %	117 %
Ω_4	31	100 %	838 %
Ω_6	127	100 %	9255 %
Ω_8	511	100 %	128161 %

Full multigrid method

- **Idea**: Improvement of the initial guess $\boldsymbol{u}^\ell$ using coarser grids
- **Vorgehensweise**:
  - Solve $\boldsymbol{A}_0 \boldsymbol{u}^0 = \boldsymbol{b}^0$ on Ω_0 exact.
  - Prolongation of $\boldsymbol{u}^0$ to Ω_1 and smoothing
    $\Rightarrow \boldsymbol{u}^1$.
  - Repeat the last step w.r.t. $\Omega_2, \ldots, \Omega_\ell$
    $\Rightarrow \boldsymbol{u}^\ell$.
  - Apply the multigrid method using $\boldsymbol{u}^\ell$
- **V-cycle** $\gamma = 1$, $l = 2$:

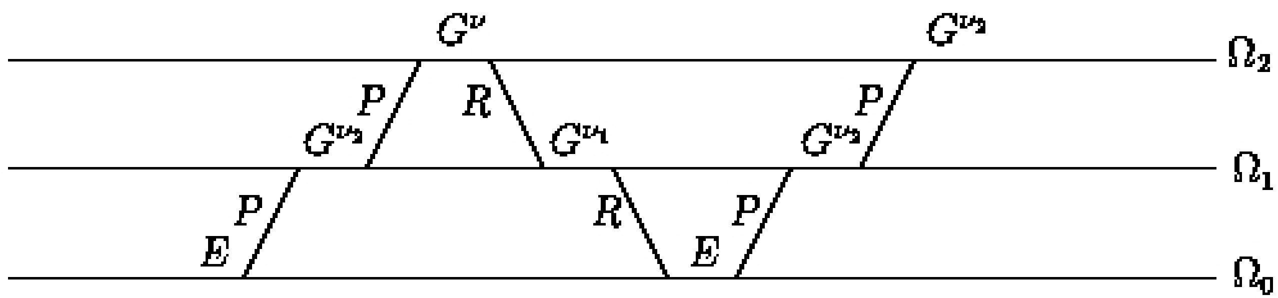

Full multigrid method - damped Jacobi method

Poisson's equation - V-cycle

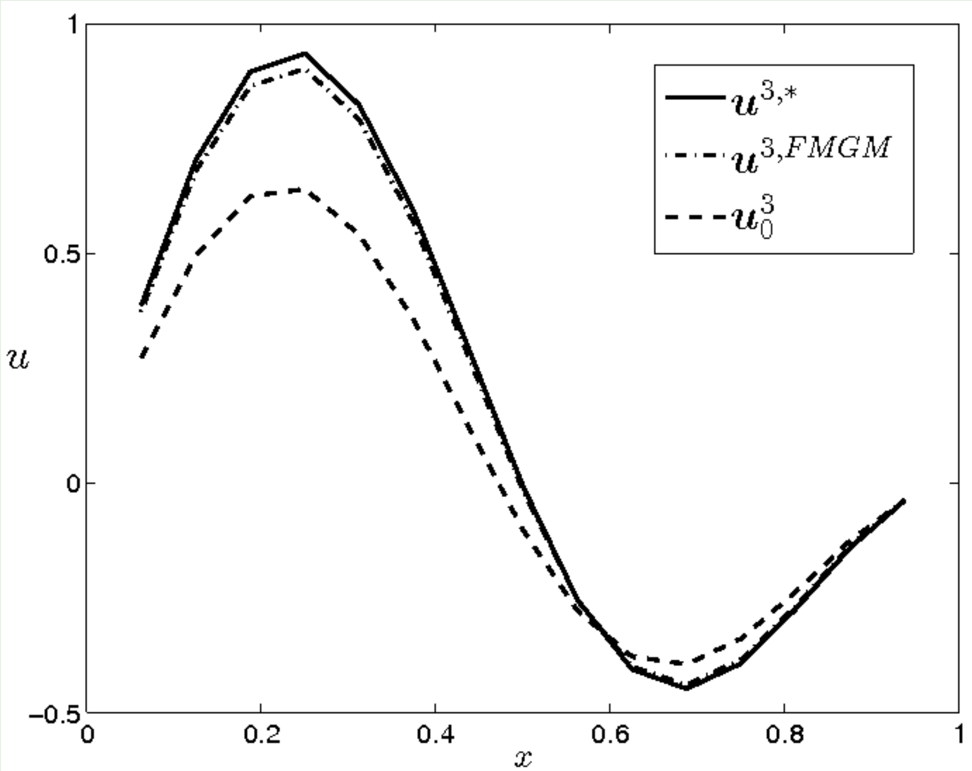

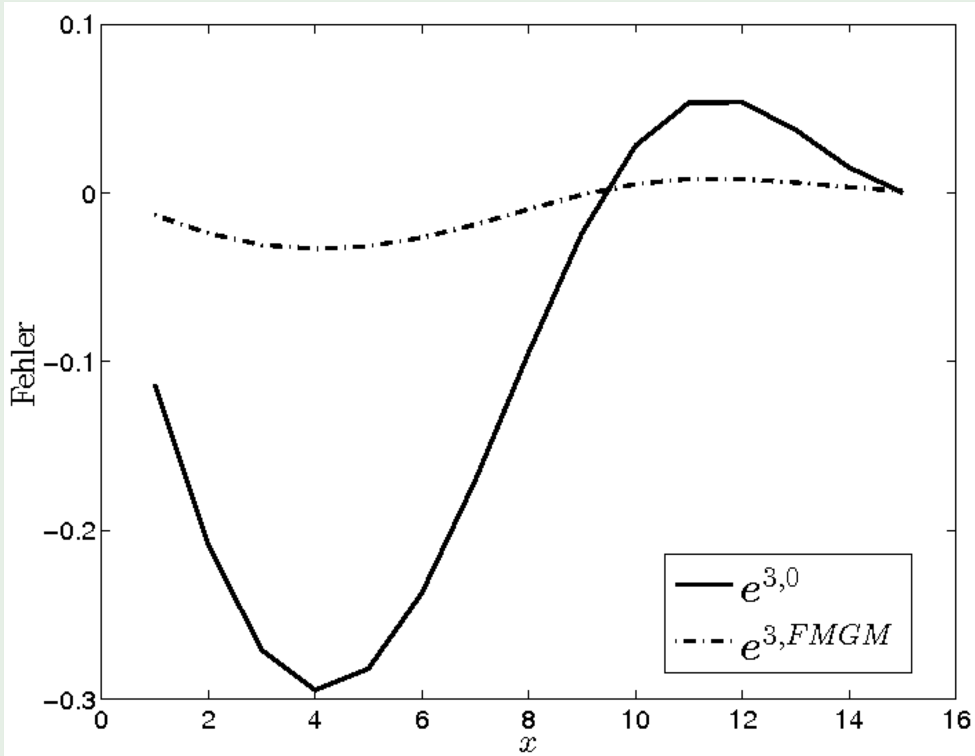

Full multigrid method - damped Jacobi method

Poisson's equation - W-cycle

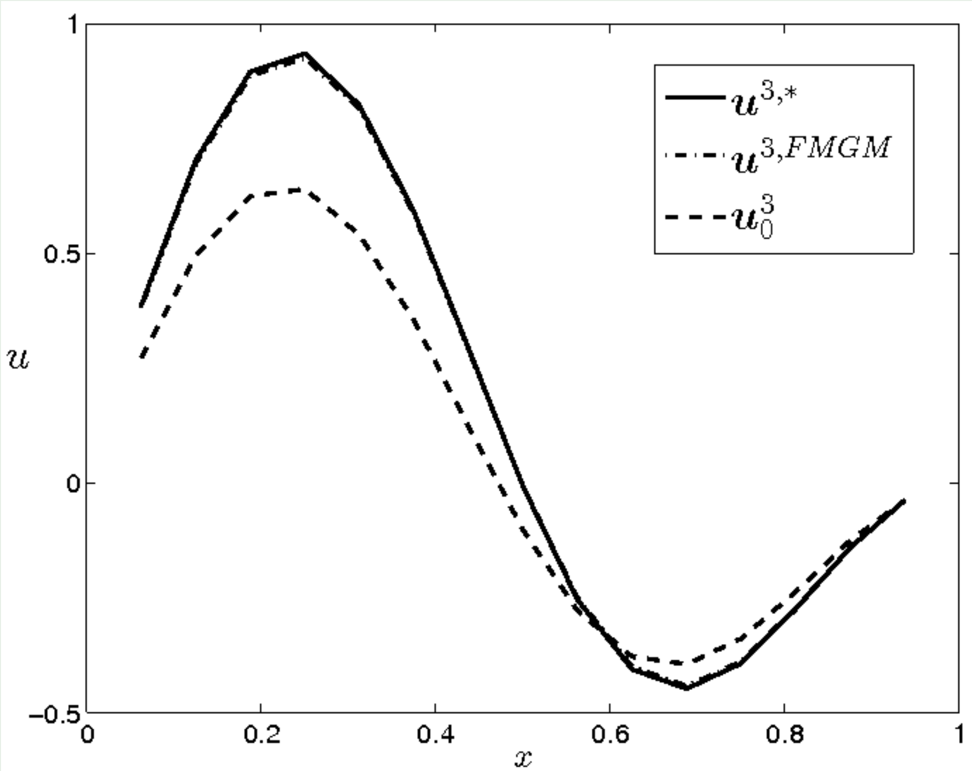

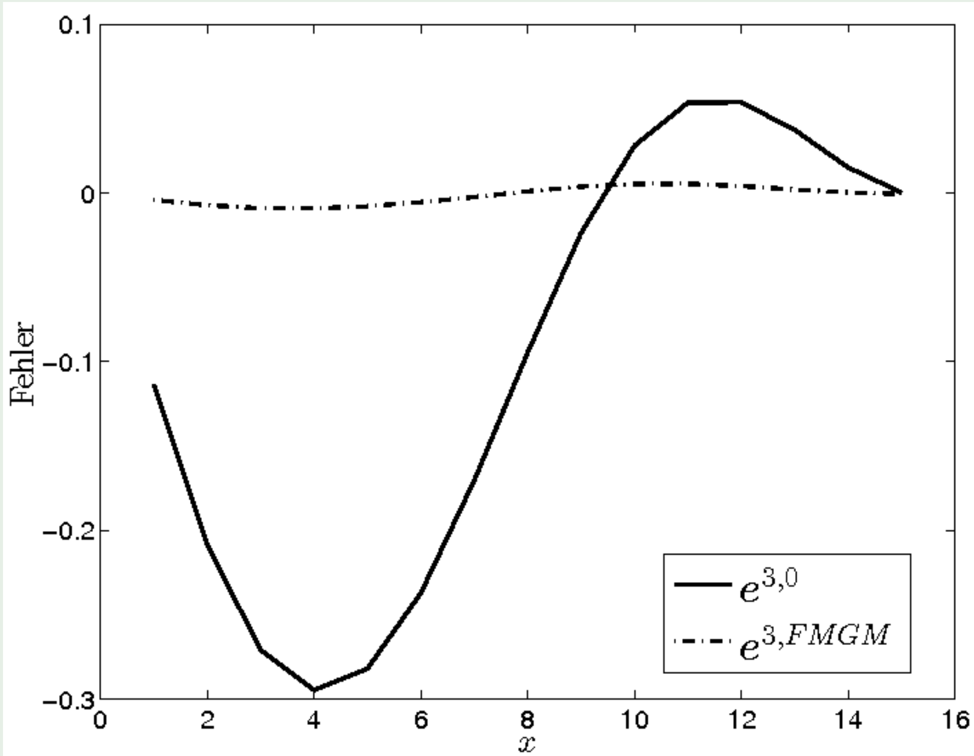

Summary

- Multigrid methods combine two algorithm with complementary properties
- Damped splitting schemes as smoother
- Coarse grid correction to handle long wave errors
- Computational effort grows linearly with the number of unknowns
- Method is much fast then usual splitting schemes
- Efficiency depends on the properties of the underlying linear system
  - Algebraic multigrid method
- Applicability as preconditioner